

## NRC Publications Archive Archives des publications du CNRC

### Analyses of post-flashover fires in a medium-sized residential room under different ventilation conditions

Saber, H. H.; Kashef, A.; Bwalya, A. C.; Loughheed, G. D.

For the publisher's version, please access the DOI link below./ Pour consulter la version de l'éditeur, utilisez le lien DOI ci-dessous.

#### **Publisher's version / Version de l'éditeur:**

<https://doi.org/10.4224/20378280>

*Research Report (National Research Council of Canada. Institute for Research in Construction); no. RR-264, 2008-10-22*

#### **NRC Publications Archive Record / Notice des Archives des publications du CNRC :**

<https://nrc-publications.canada.ca/eng/view/object/?id=7d0fba70-2e04-412f-983b-9584572a5d3b>

<https://publications-cnrc.canada.ca/fra/voir/objet/?id=7d0fba70-2e04-412f-983b-9584572a5d3b>

Access and use of this website and the material on it are subject to the Terms and Conditions set forth at

<https://nrc-publications.canada.ca/eng/copyright>

READ THESE TERMS AND CONDITIONS CAREFULLY BEFORE USING THIS WEBSITE.

L'accès à ce site Web et l'utilisation de son contenu sont assujettis aux conditions présentées dans le site

<https://publications-cnrc.canada.ca/fra/droits>

LISEZ CES CONDITIONS ATTENTIVEMENT AVANT D'UTILISER CE SITE WEB.

**Questions?** Contact the NRC Publications Archive team at

PublicationsArchive-ArchivesPublications@nrc-cnrc.gc.ca. If you wish to email the authors directly, please see the first page of the publication for their contact information.

**Vous avez des questions?** Nous pouvons vous aider. Pour communiquer directement avec un auteur, consultez la première page de la revue dans laquelle son article a été publié afin de trouver ses coordonnées. Si vous n'arrivez pas à les repérer, communiquez avec nous à PublicationsArchive-ArchivesPublications@nrc-cnrc.gc.ca.



## Analyses of Post-Flashover Fires in a Medium-Sized Residential Room Under Different Ventilations Conditions

---

**RR-264**

Saber, H.H.; Kashef, A.; Bwalya, A.C.;  
Lougheed, G.D.

October 22, 2008

The material in this document is covered by the provisions of the Copyright Act, by Canadian laws, policies, regulations and international agreements. Such provisions serve to identify the information source and, in specific instances, to prohibit reproduction of materials without written permission. For more information visit <http://laws.justice.gc.ca/en/showtdm/cs/C-42>

Les renseignements dans ce document sont protégés par la Loi sur le droit d'auteur, par les lois, les politiques et les règlements du Canada et des accords internationaux. Ces dispositions permettent d'identifier la source de l'information et, dans certains cas, d'interdire la copie de documents sans permission écrite. Pour obtenir de plus amples renseignements : <http://lois.justice.gc.ca/fr/showtdm/cs/C-42>



National Research  
Council Canada

Conseil national  
de recherches Canada

Canada



National Research  
Council Canada

Conseil national  
de recherches Canada

---

**NRC - CNRC**

---

Analyses of Post-Flashover Fires in a Medium-Sized  
Residential Room Under Different Ventilation  
Conditions

By

**Hamed H. Saber, Ahmed Kashef, Alex Bwalya and Gary Lougheed**

**Research Report # 264**

Date of Report: October 22, 2008

66 Pages

## PREFACE

This report presents the results of numerical simulations of fire development in a medium-sized residential room. The objective of this preliminary study was to evaluate the effect of various sizes and configurations of ventilation openings on fire development and thereby assist in the design of fire experiments for the Characterization of Fires in Multi-Suite Residential Dwellings (CFMRD) consortium project.

The CFMRD project is a four-year collaborative undertaking with industries, provincial governments and city authorities that was initiated by NRC-IRC in 2006 to study fires in low-rise multi-suite residential dwellings of light-frame construction. The main objectives of the project are to: a) address the lack of realistic characterized fire types, known as design fires, which are required to aid the development of methods for achieving performance-based solutions to fire problems, and b) further the understanding of how fires in residential buildings sometimes cause fatalities and substantial property losses, as revealed by fire statistics.

The CFMRD project focuses on fires in dwelling units, such as apartments, semi-detached houses, duplex houses, townhouses or row houses, secondary suites and residential care facilities as these fires have a potentially greater impact on adjacent suites.

The main tasks/deliverables of the project are:

1. To conduct fire experiments to characterize fires originating in various living spaces within multi-suite dwellings.
2. To conduct numerical simulations of various fire scenarios in order to interpolate and extend the data beyond that obtained in the experimental studies.
3. To produce a set of realistic design fires for multi-suite dwellings from the experimental data.
4. To develop an analytical method that can be used to calculate design fires for multi-suite dwellings.

The research approach employed by the project utilizes literature reviews, surveys to determine typical configurations and combustibles, computer simulations and fire experiments. A well-instrumented test facility, equipped with a calorimeter, will be used to conduct medium- and full-scale fire experiments in order to determine the combustion characteristics of typical household furnishings found in living spaces that have a high incidence of fires, individually in a single room and collectively in realistically furnished and well-instrumented simulated residential rooms. Numerical modelling of fire development, using suitable fire models, will be conducted at various stages to assist in the design and instrumentation of the full-scale fire experiments as well as to study the effect of various parameters, such as the ventilation conditions, geometry, and fire load density on the development of the fire.

# Characterization of Fires in Multi-Suite Residential Dwellings (CFMRD)

NRC-IRC gratefully acknowledges the financial and technical support of the Project Consortium, which consists of representatives from the following participating organizations:

- Canadian Automatic Sprinkler Association
- Canadian Concrete Masonry Producers Association
- Canadian Council of Furniture Manufacturers
- Canadian Wood Council
- City of Calgary
- FPInnovations - Forintek Division
- Gypsum Association
- Masonry Worx
- Ontario Ministry of Municipal Affairs and Housing
- Régie du Bâtiment du Québec
- Canadian Codes Centre

# **ACKNOWLEDGMENT**

The authors acknowledge the contribution of all of the members of the technical and advisory groups of the project at the NRC-IRC Fire Research Program: Eric Gibbs, Bruce Taber and Joseph Su.

# Analyses of Post-Flashover Fires in a Medium-Sized Residential Room Under Different Ventilation Conditions

By

Hamed H. Saber, Ahmed Kashef, Alex Bwalya and Gary Lougheed

## ABSTRACT

Establishing proper design fire scenarios is a challenging task and an essential component for conducting fire safety design of different buildings. A design fire scenario is a qualitative description of a fire with time identifying key events that characterize the fire (ignition, growth, fully-developed, and decay stages of a fire). In addition, it describes the ventilation conditions that will impact the course of a fire. A number of fire ventilation scenarios were investigated in order to identify the proper ventilation scheme for conducting design fire tests in a compartment of a size 4.2 m long, 3.8 m wide, and 2.4 m high. This effort is a part of the process of designing fire experiments in a project concerning the characteristics of fires in various rooms in low-rise residential dwelling units of light-frame construction. The fuel package that was used in all scenarios consisted of a mock-up sofa and two wood cribs underneath it. The mock-up sofa was constructed entirely out of flexible polyurethane foam. The two wood cribs provided additional fuel load to sustain a fully-developed fire. The selection of this fuel package is supported by fire statistics that many fatal residential fires begin with an item of upholstered furniture.

The fire characteristics of nine ventilation scenarios (SC1 through SC9) are available in the previous report [1] which describes flow fields within the compartment, flow through the opening(s), location of the neutral plane(s) in the opening(s), the heat release rate, shapes and sizes of the flames. In this report, two more ventilation scenarios (SC10 and SC11) were conducted in order to cover ventilation- and fuel-controlled burning in a room of a size of 4.2 m long, 3.8 m wide and 2.4 m high. Furthermore, the effect of window opening size, doorway size, and fire load location on the heat release rate, period of burning, remaining mass of the fire load, effective heat of combustion, temperature during the period of fully-developed fire (post-flashover), onset of post-flashover, and period of post-flashover were investigated.

The Computational Fluid Dynamics (CFD) technique was used to conduct the numerical simulations for all ventilation scenarios using the Fire Dynamics Simulator (FDS) version 5 [6]. Unlike the previous versions of FDS, the new combustion model in the FDS version 5 accounts for both mixing of fuel and oxygen without burning and the CO production (incomplete combustion). These are important features for the proper modelling of under-ventilated fires. The CFD simulations conducted in this study will assist in the design of medium and large-scale fire tests to be conducted to evaluate various fire scenarios. In a later stage of this project, the CFD model will be used to conduct parametric studies to determine the effect of various parameters, such as the ventilation conditions, geometry, and type of fire load on the fire development. This information will be used to evaluate the impact of a fire on the life safety, structure integrity, and property protection.

## Table of Contents

<b>Preface .....</b>	<b>ii</b>
<b>1 Introduction .....</b>	<b>1</b>
<b>2 CFD Simulation.....</b>	<b>7</b>
<b>3 Results and Discussions .....</b>	<b>10</b>
3.1 Temporal Change in Heat Release Rate .....	11
3.2 Effect of Window Opening Size on Fire Characteristics .....	14
Ventilation scenarios using one window opening with different sizes .....	14
Ventilation scenarios using a window opening and doorway in the opposite walls.	18
Ventilation scenarios using a window opening and doorway in the same wall .....	21
3.3 Effect of Doorway Size on Fire Characteristics .....	22
3.4 Effect of Fire Location on Fire Characteristics .....	26
3.5 Stage of Fully-Developed Fire (Post-flashover) .....	31
Babrauskas' correlation for post-flashover .....	31
Temperature and mass loss during post-flashover stage .....	34
Comparison of post-flashover temperatures of different scenarios.....	36
<b>4 Summary and Conclusion .....</b>	<b>43</b>
<b>5 References .....</b>	<b>45</b>
<b>6 Appendix–A: Average Temperatures and Mass Losses within the Period of Post-flashover for all Ventilation Scenarios .....</b>	<b>46</b>

## List of Figures

Figure 1-1 Room size and fire load [1] .....	2
Figure 1-2 Ventilation parameters for scenarios using a window opening (different sizes) .....	4
Figure 1-3 Ventilation parameters for scenarios using a window opening (different sizes) and doorway (same size) facing each other .....	5
Figure 1-4 Ventilation parameters for scenarios using a window opening (different sizes) and doorway (same size) in the same wall .....	5
Figure 1-5 Ventilation parameters for scenarios using a doorway (different sizes) .....	6
Figure 1-6 Ventilation parameters for scenarios using a window opening (same size) and different fire load locations .....	6
Figure 2-1 Stretched mesh in the x- and y-directions to capture the important phenomena. ....	9
Figure 2-2 A schematic of the calculated flame cross-section for a given mesh and the actual flame surface .....	10
Figure 3-1 Heat Release Rate of ventilation scenario SC1 (window opening 1.5x1.5 m) .....	12
Figure 3-2 Comparison of the HRRs for ventilation scenarios using one window opening with different sizes.....	13
Figure 3-3 Status of the wood cribs at the time at which the polyurethane sofa was completely burned in SC1, SC3, SC10 and SC11 .....	15
Figure 3-4 Status of the wood cribs when the burning stopped in SC1, SC3 & SC11 (HRR = ~1 kW) and at the end of simulation in SC10 (HRR ~ 1500 kW at 900 s) .....	16
Figure 3-5 Comparison of the HRRs for ventilation scenarios using window opening (different sizes) and doorway (same size) facing each other .....	17
Figure 3-6 Status of the wood cribs at time at which the polyurethane sofa was completely burned in SC2 and SC4 .....	19
Figure 3-7 Status of the wood cribs when the burning stopped in SC2 and SC4 (HRR = ~1 kW).....	19
Figure 3-8 Comparison of the HRRs for ventilation scenarios using window opening (different sizes) and doorway (same size) located in the same wall side .....	20
Figure 3-9 Status of the wood cribs at time at which the polyurethane sofa was completely burned in SC7 and SC8 .....	21
Figure 3-10 Status of the wood cribs when the burning stopped in SC7 and SC8 (HRR = ~1 kW).....	22
Figure 3-11 Comparison of the HRRs for ventilation scenarios using a doorway with different sizes .....	24
Figure 3-12 Status of the wood cribs at time at which the polyurethane sofa was completely burned in SC5 and SC6 .....	25
Figure 3-13 Status of the wood cribs when the burning stopped in SC5 and SC6 (HRR = ~1 kW).....	25
Figure 3-14 Comparison of the HRRs for ventilation scenarios using same window opening size and different fire load locations .....	27
Figure 3-15 Status of the wood cribs at time at which the polyurethane sofa was completely burned in SC3 and SC9 .....	28
Figure 3-16 Status of the wood cribs when the burning stopped in SC3 and SC9 (HRR = ~1 kW).....	28

Figure 3-17 Comparison of the average temperature over the period of post-flashover with that obtained using Babrauskas' correlation [11] for all scenarios.....	33
Figure 3-18 Comparison of the average temperatures and mass losses during the period of post-flashover for scenarios using a window opening with different sizes .....	37
Figure 3-19 Comparison of the average temperatures and mass losses during the period of post-flashover for scenarios using window opening and doorway facing each other .	38
Figure 3-20 Comparison of the average temperatures and mass losses during the period of post-flashover for scenarios using window opening and doorway located in the same wall .....	39
Figure 3-21 Comparison of the average temperatures and mass losses during the period of post-flashover for scenarios using doorway with different sizes .....	40
Figure 3-22 Comparison of the average temperatures and mass losses during the period of post-flashover for scenarios with different fire load locations.....	41
Figure 3-23 Average temperature of all ventilation scenarios over the period of post-flashover.....	42
Figure 6-1 Temperature and mass loss during the period of post-flashover for ventilation scenario SC1.....	47
Figure 6-2 Temperature and mass loss during the period of post-flashover for ventilation scenario SC2.....	48
Figure 6-3 Temperature and mass loss during the period of post-flashover for ventilation scenario SC3.....	49
Figure 6-4 Temperature and mass loss during the period of post-flashover for ventilation scenario SC4.....	50
Figure 6-5 Temperature and mass loss during the period of post-flashover for ventilation scenario SC5.....	51
Figure 6-6 Temperature and mass loss during the period of post-flashover for ventilation scenario SC6.....	52
Figure 6-7 Temperature and mass loss during the period of post-flashover for ventilation scenario SC7.....	53
Figure 6-8 Temperature and mass loss during the period of post-flashover for ventilation scenario SC8.....	54
Figure 6-9 Temperature and mass loss during the period of post-flashover for ventilation scenario SC9.....	55
Figure 6-10 Temperature and mass loss during the period of post-flashover for ventilation scenario SC10 .....	56
Figure 6-11 Temperature and mass loss during the period of post-flashover for ventilation scenario SC11 .....	57

## List of Tables

Table 1-1 Ventilation conditions for all scenarios.....	3
Table 1-2 Mass of fire load used in all ventilation scenarios [1].....	3
Table 3-1 Comparison of the maximum HRR and burning rate of all scenarios .....	29
Table 3-2 Comparison of the time and burned mass when sofa completely burned .....	30
Table 3-3 Comparison of the total mass losses, total energy release and the effective heat of combustion.....	30
Table 3-4 Calculated average temperature over the period of post-flashover based on CFD simulations and Babrauskas' correlation [11] for all scenarios .....	33

# 1 Introduction

This report documents the analyses for a series of CFD numerical simulations that were conducted in order to study the effect of ventilation settings on fire dynamics in a room of a size of 4.2 m long, 3.8 m wide and 2.4 m high. The fire was initiated by igniting an item of upholstered furniture. A fuel package consisted of a mock-up sofa constructed with exposed polyurethane foam, the dominant combustible constituent of upholstered furniture, and two wood cribs. The mock-up sofa was ignited first and the wood cribs provided the remaining fire load to sustain a fully-developed fire. The details of the fuel package and its characteristics are available in [1 – 5]. This mode of fire initiation is supported by fire statistics that many fatal residential fires begin with upholstered furniture.

Eleven CFD simulations for different ventilation scenarios were investigated in order to identify the proper ventilation scheme for conducting design fire tests. These scenarios covered a wide range of ventilation factor,  $\Psi$ , of  $\sim 0.01 - 0.08 \text{ m}^{1/2}$ , ( $\Psi = A_o \sqrt{H_o} / A_T$ , where  $A_o$  = area of the opening(s),  $A_T$  = total surface area of the compartment, and  $H_o$  = weighted average of the opening(s) height). In this ventilation range, both ventilation-controlled and fuel-controlled burning were covered. This report extends the previous effort [1] with a focus on:

- (a) Investigating the effect of window opening size on the fire characteristics (in terms of heat release rate, period of burning, remaining mass of the fire load, effective heat of combustion, temperature, onset of fully-developed fire (post-flashover), period of post-flashover, etc) for ventilation scenarios using: (1) one window opening with different sizes (Figure 1-2), (2) a window opening and doorway in opposite walls (Figure 1-3), and (3) a window opening and doorway in the same wall (Figure 1-4),
- (b) Investigating the effect of doorway size on the fire characteristics (Figure 1-5),
- (c) Investigating the effect of fire location on the fire characteristics (Figure 1-6), and
- (d) Comparing the average temperature over the period of post-flashover for a wide range of ventilation factor,  $\Psi$ .

In all CFD simulations, the fire load that was used consisted of a polyurethane sofa and two wood cribs (Figure 1-1 and Table 1-1). The dimensions and thermal properties of the polyurethane sofa and wood cribs are available in reference [1]. In the next phase, after identifying the proper ventilation scheme and conducting tests, the numerical results will be compared with experimental results. After verifying the CFD simulation, a parametric analysis will be performed to investigate the effect of different parameters of interest (e.g. fire size, fire location, geometry, etc).

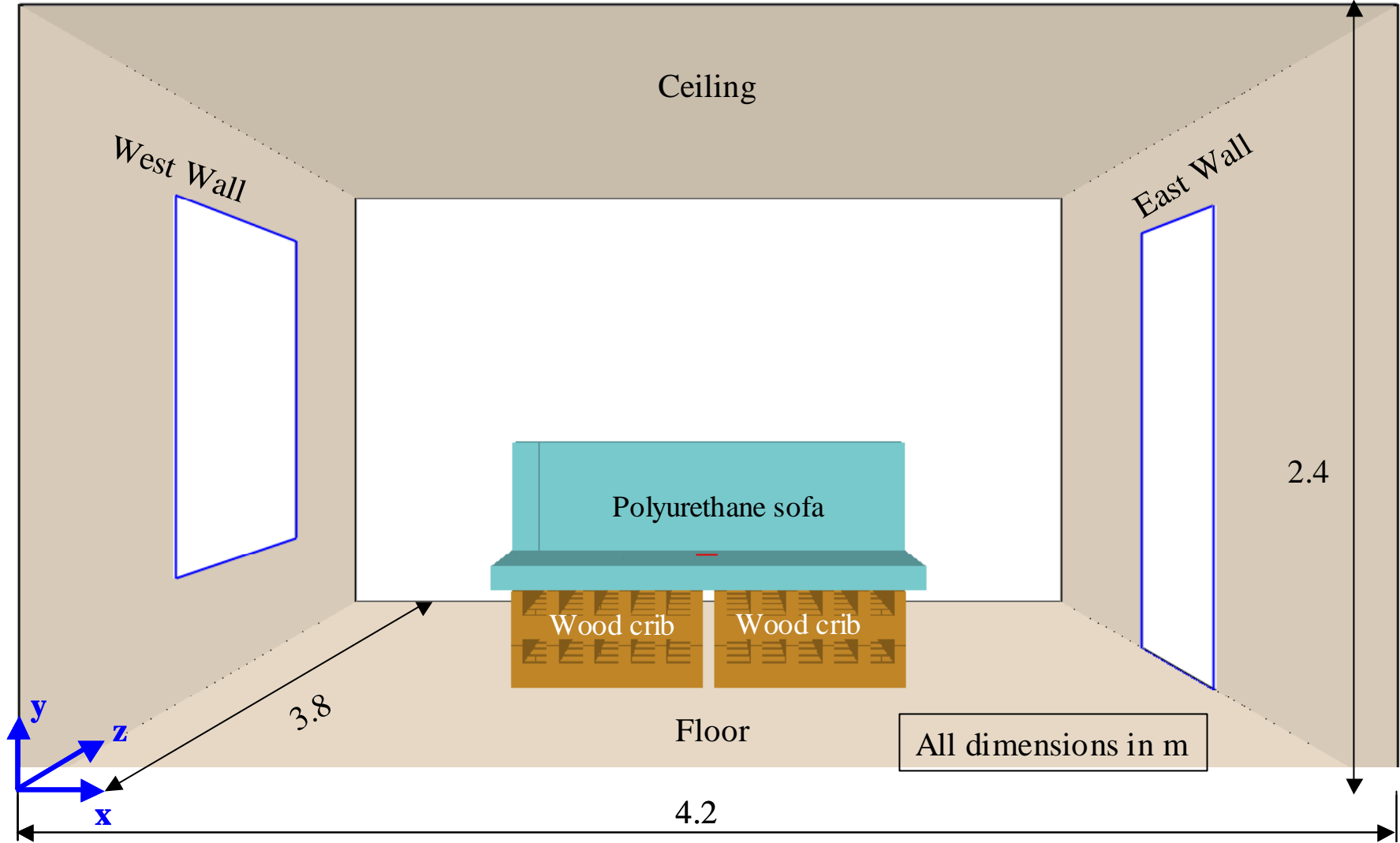


Figure 1-1 Room size and fire load [1]

Table 1-1 Ventilation conditions for all scenarios

Ventilation Scenario	Window Opening Size (m)		Doorway Size (m)		Window Opening Location		Doorway Location		Fire Load Location
	Width	Height	Width	Height	Side	Center (x,y,z) (m)	Side	Center (x,y,z) (m)	
<b>SC1</b>	1.5	1.5	Closed		West	(0,1.9,1.25)	Closed		Center of room
<b>SC2</b>	1.5	1.5	0.9	2.0	West	(0,1.9,1.25)	East	(4.2,1.9,1.0)	Center of room
<b>SC3</b>	2.0	1.5	Closed		West	(0,1.9,1.25)	Closed		Center of room
<b>SC4</b>	1.0	1.0	0.9	2.0	West	(0,1.9,1.5)	East	(4.2,1.9,1.0)	Center of room
<b>SC5</b>	Closed		0.9	2.0	Closed		East	(4.2,1.9,1.0)	Center of room
<b>SC6</b>	Closed		1.5	2.0	Closed		East	(4.2,1.9,1.0)	Center of room
<b>SC7</b>	1.0	1.5	0.9	2.0	East	(4.2,2.85,1.25)	East	(4.2,0.95,1.0)	Center of room
<b>SC8</b>	1.0	1.0	0.9	2.0	East	(4.2,2.85,1.5)	East	(4.2,0.95,1.0)	Center of room
<b>SC9</b>	2.0	1.5	Closed		West	(0,1.9,1.25)	Closed		Corner of room*
<b>SC10</b>	1.0	1.0	Closed		West	(0,1.9,1.0)	Closed		Center of room
<b>SC11</b>	1.4	1.2	Closed		West	(0,1.9,1.1)	Closed		Center of room

\* Fire load was separated by 0.10 m from the east and north walls

Table 1-2 Mass of fire load used in all ventilation scenarios [1]

Ventilation scenario	Polyurethane sofa mass (kg)	Number of wood cribs	Wood moisture content (%w)	Total wood mass (kg)
SC1 through SC11	8.3	2	10	86.7

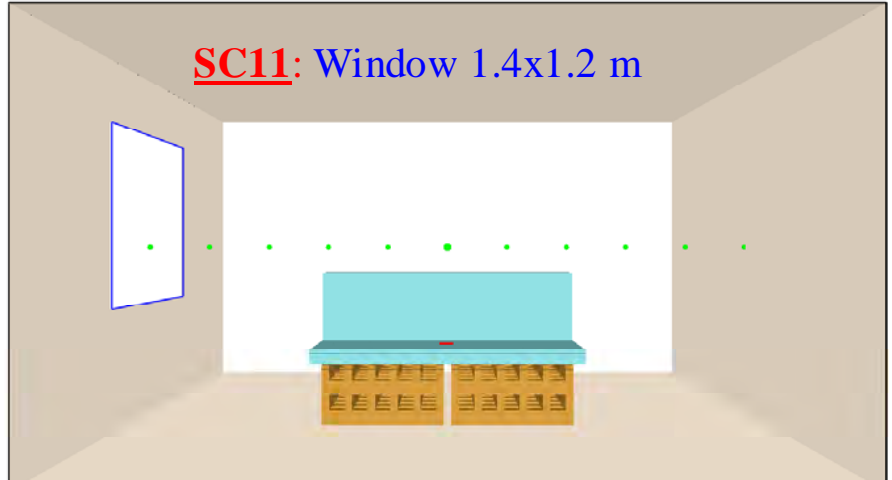
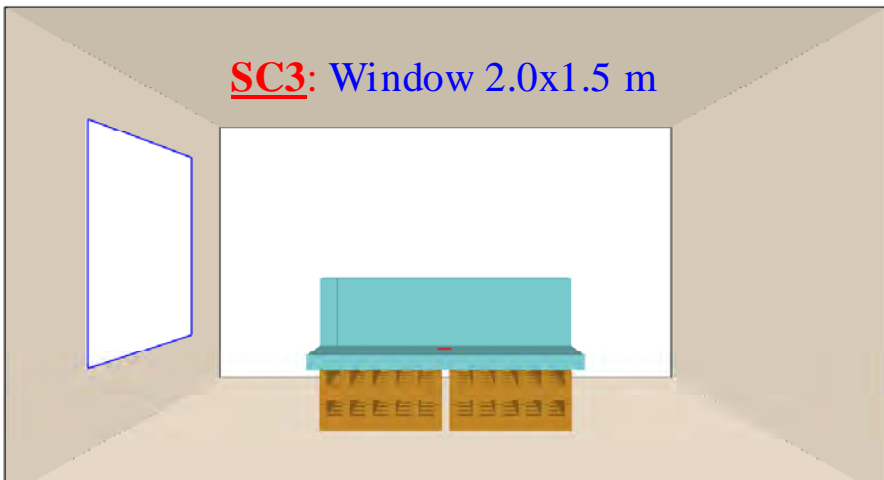
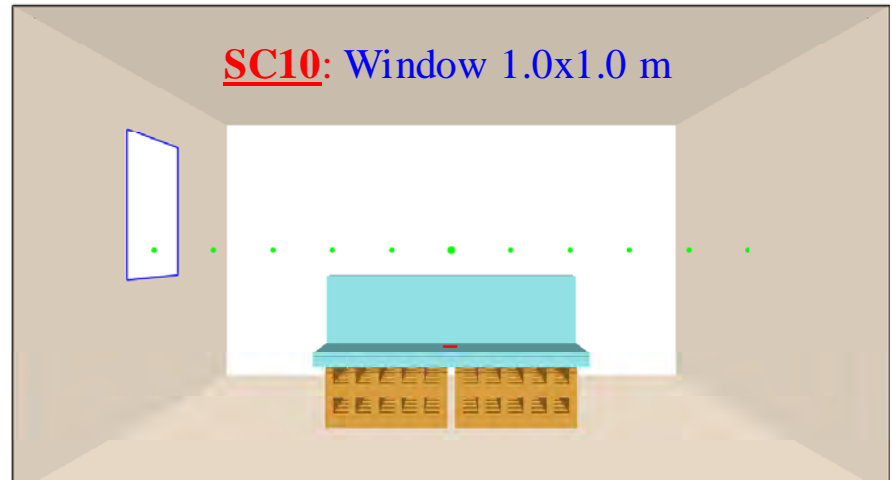
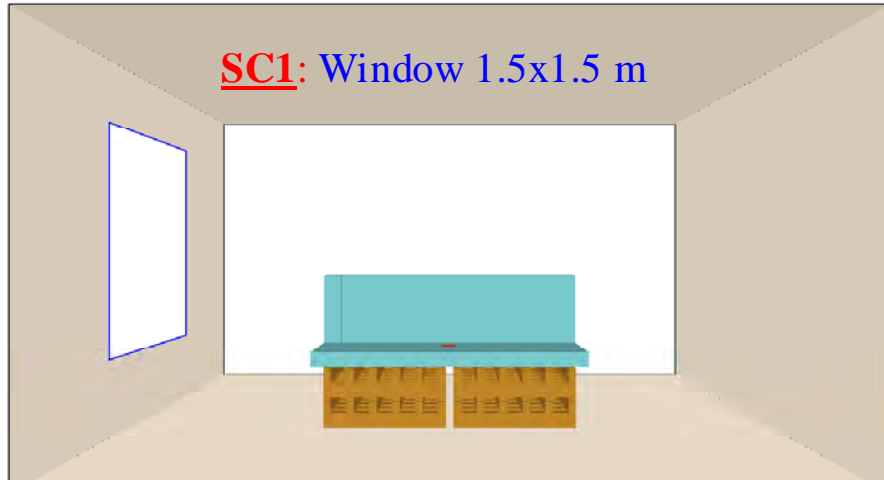


Figure 1-2 Ventilation parameters for scenarios using a window opening (different sizes)



Figure 1-3 Ventilation parameters for scenarios using a window opening (different sizes) and doorway (same size) facing each other

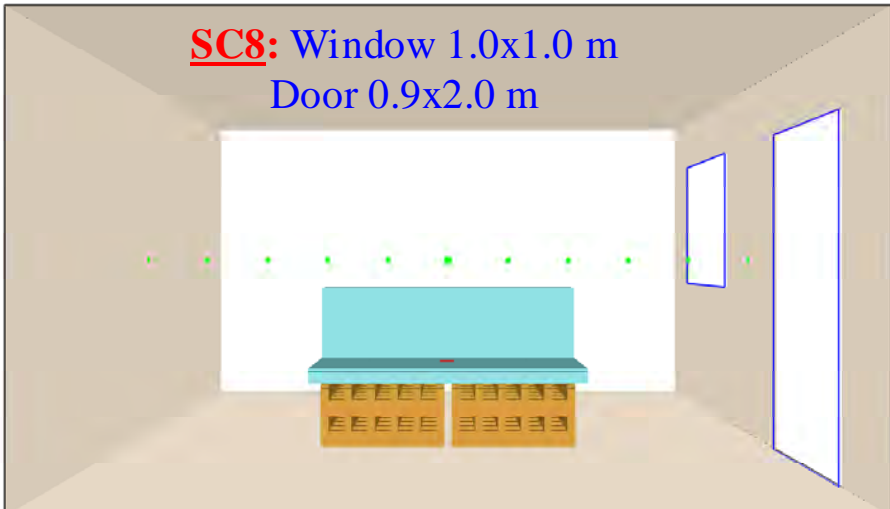
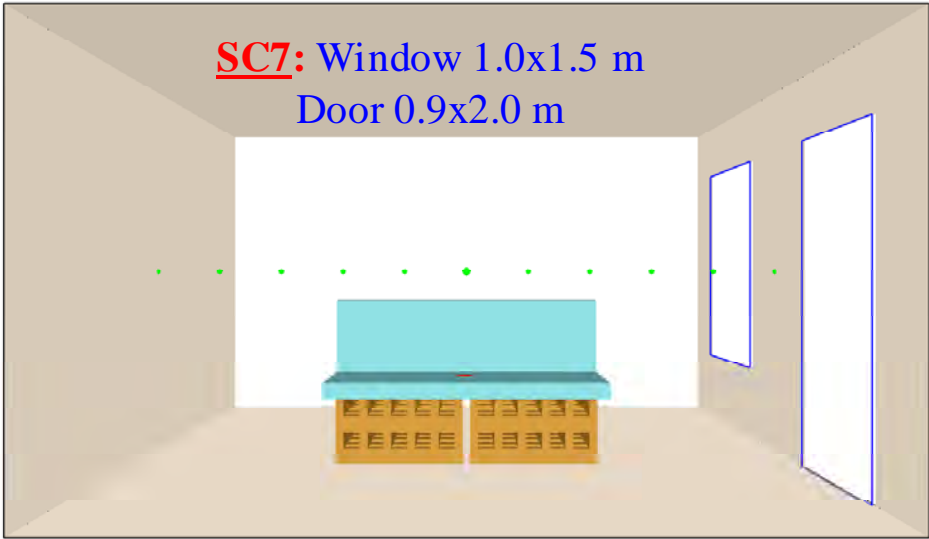


Figure 1-4 Ventilation parameters for scenarios using a window opening (different sizes) and doorway (same size) in the same wall

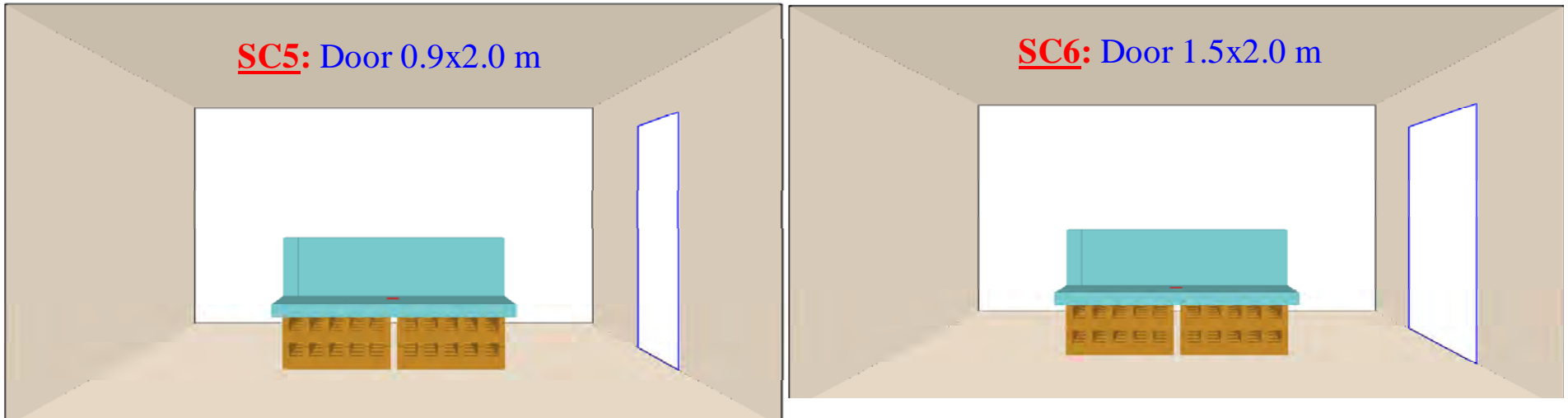


Figure 1-5 Ventilation parameters for scenarios using a doorway (different sizes)

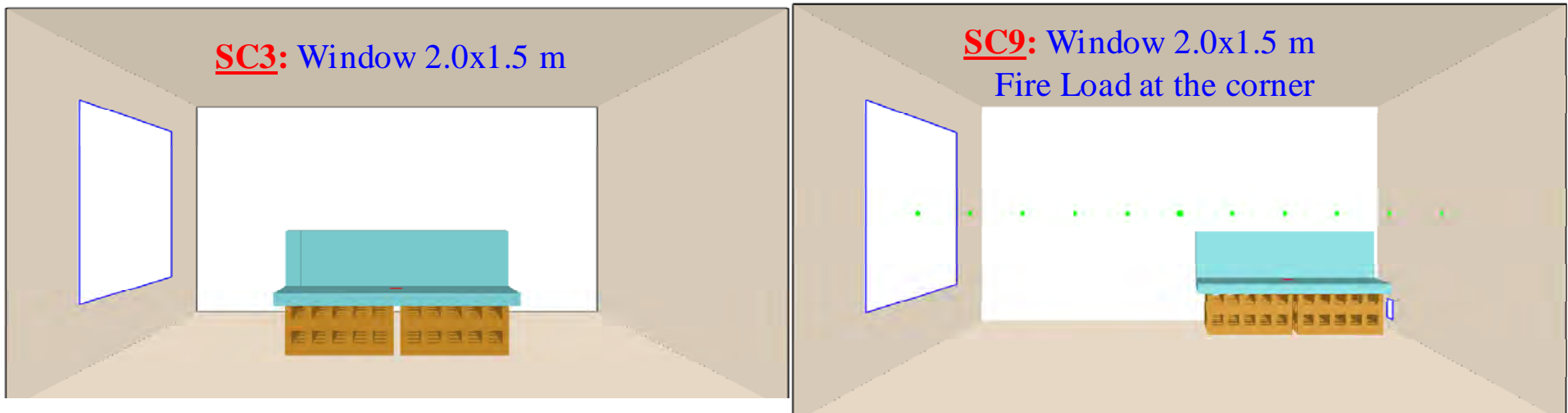


Figure 1-6 Ventilation parameters for scenarios using a window opening (same size) and different fire load locations

## 2 CFD Simulation

The Fire Dynamic Simulator (FDS) is a Computational Fluid Dynamics (CFD) model developed to idealize fire-driven fluid flow. The model numerically solves a form of the Navier-Stokes equations appropriate for low-speed, thermally driven flow, with an emphasis on smoke and heat transport from fires. The partial differential equations for conservation of mass, momentum, and energy are discretized using the finite difference method, and the solution is updated in time on a three-dimensional, rectilinear grid. Thermal radiation is computed using a finite volume technique on the same grid as the flow solver. Lagrangian particles are used to simulate smoke movement and sprinkler discharge. FDS computes the temperature, density, pressure, velocity, and chemical composition within each numerical grid cell at each discrete time step. FDS computes the temperature, heat flux, mass loss rate, and various other quantities at solid surfaces.

Version 5 of FDS [6-7] was used to simulate the eleven ventilation scenarios listed in Table 1-1 in a room of a size of 4.2 x 3.8 x 2.4 m (Figure 1-1). Grids or meshes were developed in which the volume within the room was divided into hundreds of thousands of control volumes or cells. In each cell, the governing equations (momentum, energy, and diffusion equations) are simultaneously solved for velocities, temperatures and mass fractions as a function of time. Only one mesh (stretched in x- and y-directions, and uniform in z-direction) was designed for each ventilation scenario. The total number of cells was 720,000. As shown in Figure 2-1, the mesh was refined in the regions where large temporal and/or spatial gradients of key flow quantities are anticipated (e.g. in the vicinity of the fire, doorway and window opening). In order to capture the steep change of the key quantities with time, the time step ( $\Delta t$ ) was selected according:

$$\Delta t = \min[(\Delta x, \Delta y, \Delta z)^2 / \alpha], \quad (2-1)$$

where  $\alpha$  is the thermal diffusivity [ $\alpha = k / (\rho C_p)$ ], and  $\Delta x$ ,  $\Delta y$ ,  $\Delta z$  are the cell size in x-, y- and z-directions, respectively. Note that, the local heat release rate (HRR) was calculated from the local oxygen consumption rate at the flame surface. Therefore, a fine mesh is necessary where the flame exists in order to capture the profile of the flame surface (see Figure 2-2), and hence accurately predict the HRR. The CPU time using the NRC-IRC cluster machine for each scenario was ~14 – 21 days.

The walls, floor and ceiling of the room were assumed inert and perfectly insulated (adiabatic) in all scenarios. This represented the case of most severe fire conditions. In all scenarios, the window openings and doorways were leading to the exterior (i.e. open to the outside), meaning that the inflow to the compartment is fresh air at ambient conditions. Ventilation vents were introduced to mimic the doorways and window openings as shown in Figure 1-2 through Figure 1-6 and Table 1-1. The total local pressure (dynamic + static + gravitational pressure) in the room with and without fire is equal to the atmospheric pressure. To satisfy this condition, the boundary conditions at the window openings and doorways were treated as open vents. Upon initiating the fire, the flow field inside the room will be modified such that the total local pressure in the room will equal the atmospheric pressure. Subsequently, the mass flow rates at the doorways and window openings were calculated and these values were different depending on the ventilation scenario. The eleven fire simulations were conducted for a

period of 900 s. The CFD simulation in each scenario was terminated after the combustion process was completely stopped. As will be shown later, the combustion of the fire load was completely stopped at different periods of time for these ventilation scenarios.

Unlike the previous versions of FDS, the new combustion model in the FDS version 5 accounts for both mixing of fuel and oxygen without burning and the CO production (incomplete combustion). These are important features for the proper modelling of under-ventilated fires. Before conducting the CFD simulations for all scenarios, many numerical tests and debugging were carried out in order to (a) find out the optimum mesh size, and (b) test the validity of the new combustion model in FDS version 5 (see reference [1] for more details).

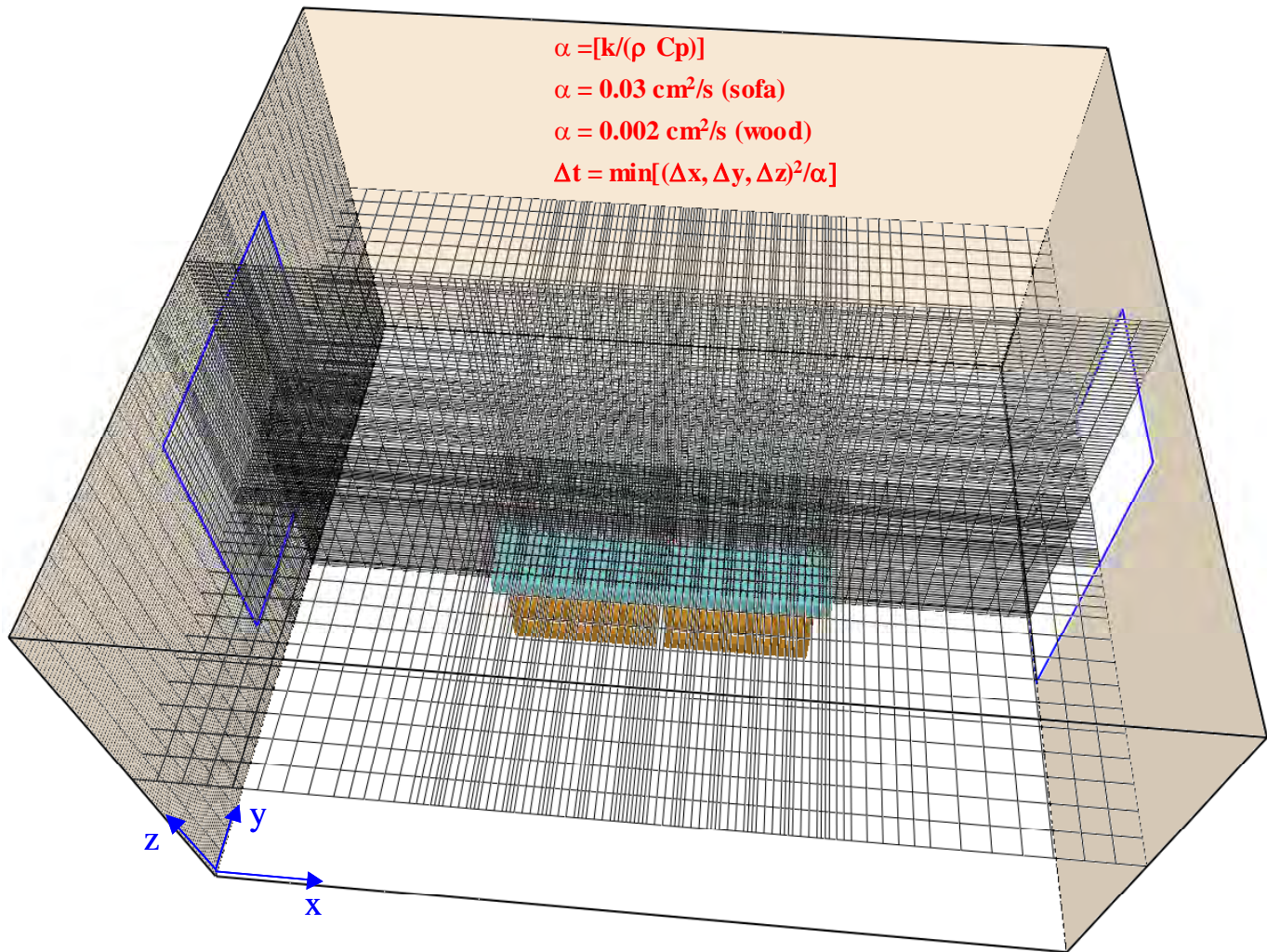


Figure 2-1 Stretched mesh in the x- and y-directions to capture the important phenomena.

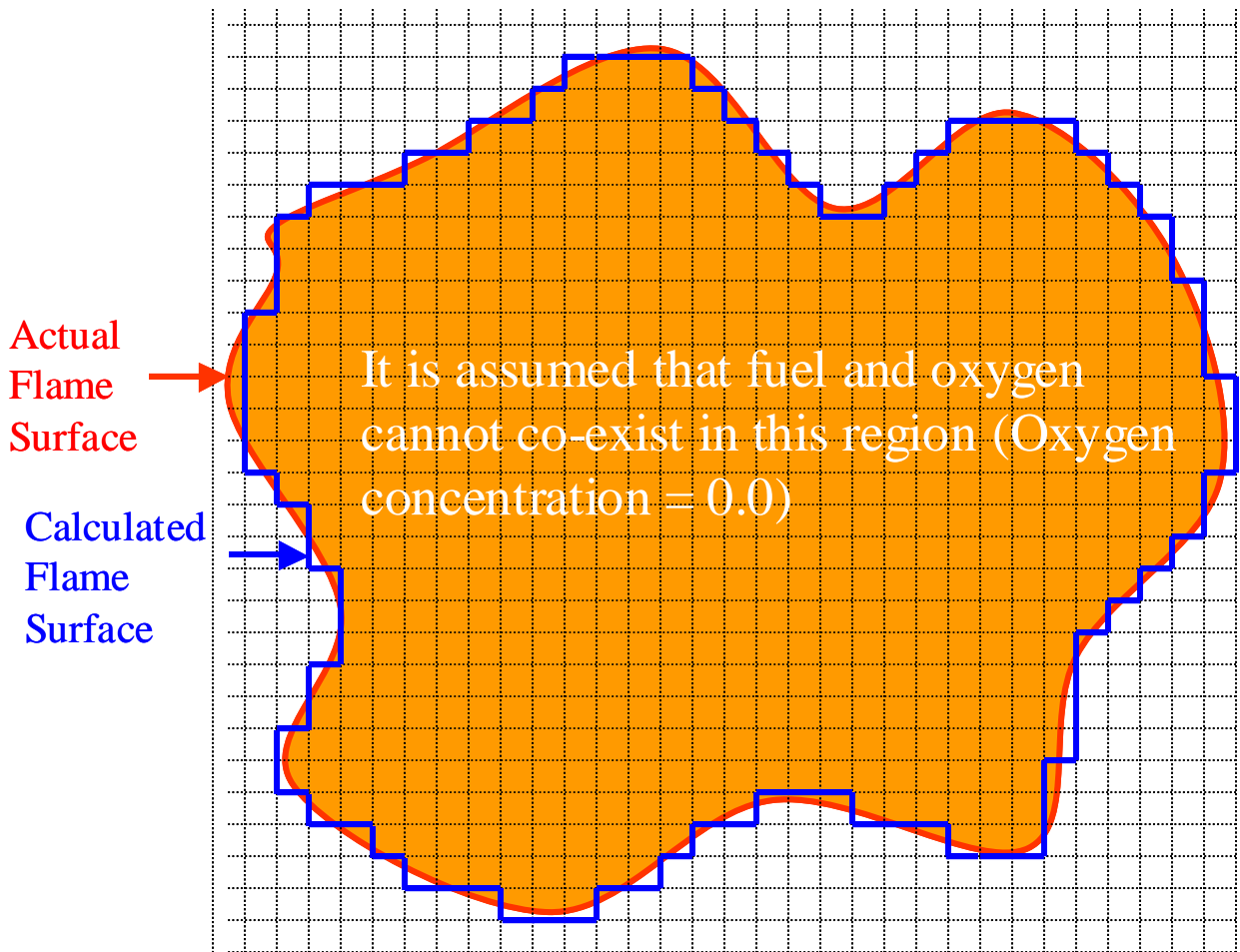


Figure 2-2 A schematic of the calculated flame cross-section for a given mesh and the actual flame surface

### 3 Results and Discussions

In this section, the results of the different ventilation scenarios are presented and discussed. The fire characteristics of ventilation scenarios SC1 through SC9 are available in the previous report [1], which describes flow fields within the compartment, flow through the opening(s), location of the neutral plane(s) in the opening(s), heat release rate, shapes and sizes of the flames. In this report, two more ventilation scenarios (SC10 and SC11) were conducted in order to cover ventilation- and fuel-controlled burning. Scenario SC10 had a square window opening of a size of 1.0 m. Scenario SC11 had a 1.4 m wide and 1.2 m high rectangular window opening, which is the average size of window openings in multi-family dwellings based on a survey that was conducted recently [3]. In the next subsections, the effect of window opening size, doorway size and fire location on the heat release rate, period of burning, remaining mass of the fire load, effective heat of combustion, temperature during the period of fully-developed fire (post-flashover), onset of post-flashover, and period of post-flashover are discussed.

### 3.1 Temporal Change in Heat Release Rate

An example for heat release rate (HRR) is shown in Figure 3-1 for scenario SC1. Snapshots for flame shapes at different times are shown in inserts (a) through (f) of Figure 3-1. As shown in this figure, the HRR increased rapidly with time and reached its maximum value (6,092 kW) at 24 s. At this time the size of the flame was large and filled a significant portion of the room (insert a). After 24 s, the HRR decreased rapidly with time until 37 s. In the period from 37 s to 236 s, the HRR was more or less constant and its mean value was 3,850 kW. In this period, the size of the flame was smaller (insert b, c) than that at 25 s (insert a), and the HRR was due to burning both the polyurethane sofa and wood cribs. In the period from 236 s to 269 s, the HRR was approximately constant (its mean value equal 3,965 kW). After 269 s, the HRR decreased with time, reaching its minimum value (479 kW) at 325 s. At this time (325 s), the size of the flame reached its minimum size and the majority of the HRR was due to burning of the wood crib that was located further from the window opening (see insert d). After that the HRR and the flame size increased again with time, reaching another peak (2,347 kW, insert e) at 400 s. In the period from 400 s – 425 s, the HRR decreased slowly with time. For example, the HRR decreased from 2,347 kW to 2,211 kW as the time increased from 400 s to 425 s. After 425 s, the HRR decreased rapidly. Eventually, the HRR decreased to ~1 kW at 600 s (see the amount of wood remaining in the insert (g) in Figure 3-1). In the later stages of burning, the predicted flame size above the wood crib located further from the window opening was larger than that above the wood crib located closer to the window opening (e.g. see the inserts d, e, f). As a result, the amount of mass loss from the wood crib located further from the window opening was greater than that from the wood crib located closer to the window opening as shown in the insert (g). A similar trend for the HRR and predicted flame shapes were obtained for other ventilation scenarios.

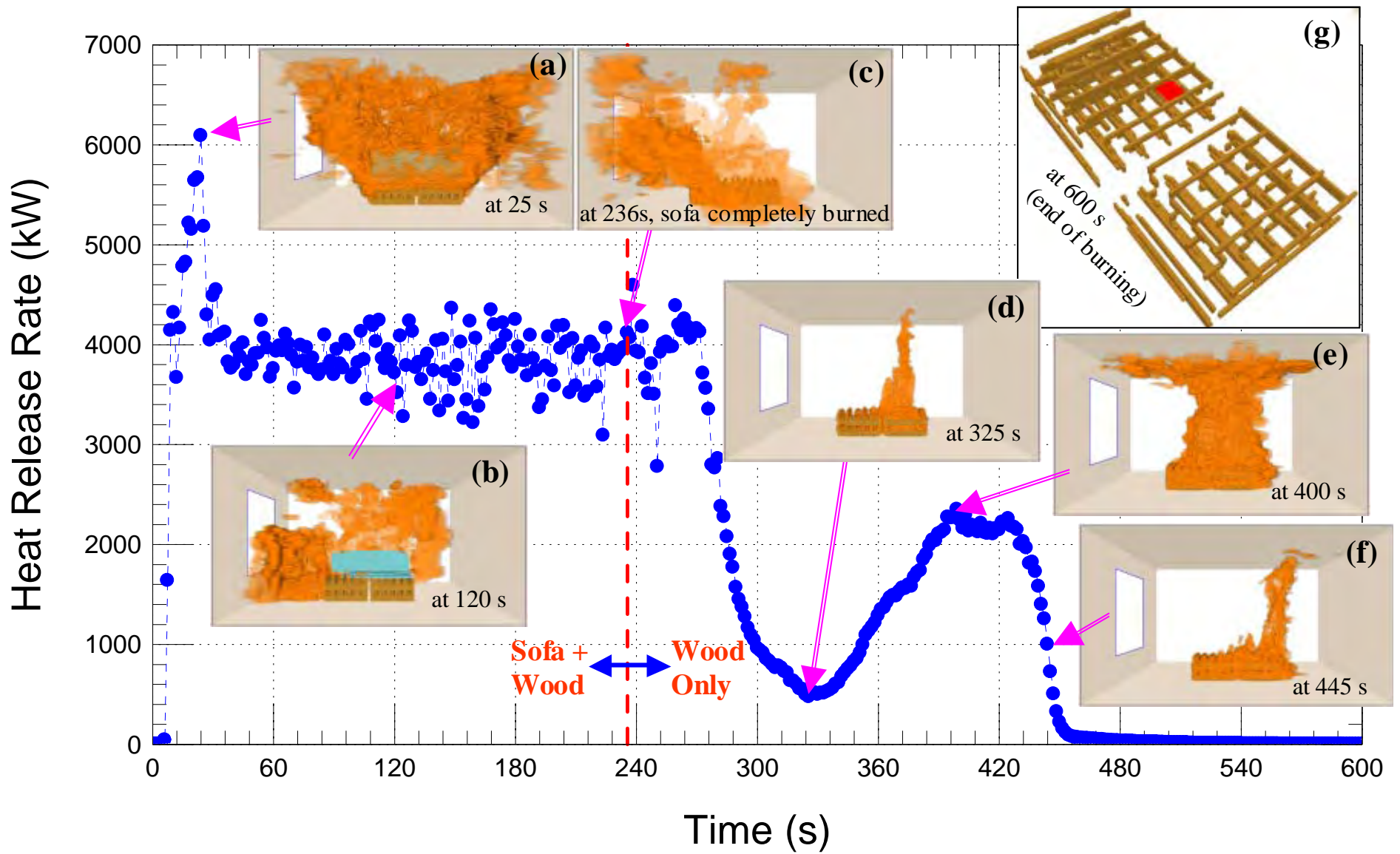


Figure 3-1 Heat Release Rate of ventilation scenario SC1 (window opening 1.5x1.5 m)

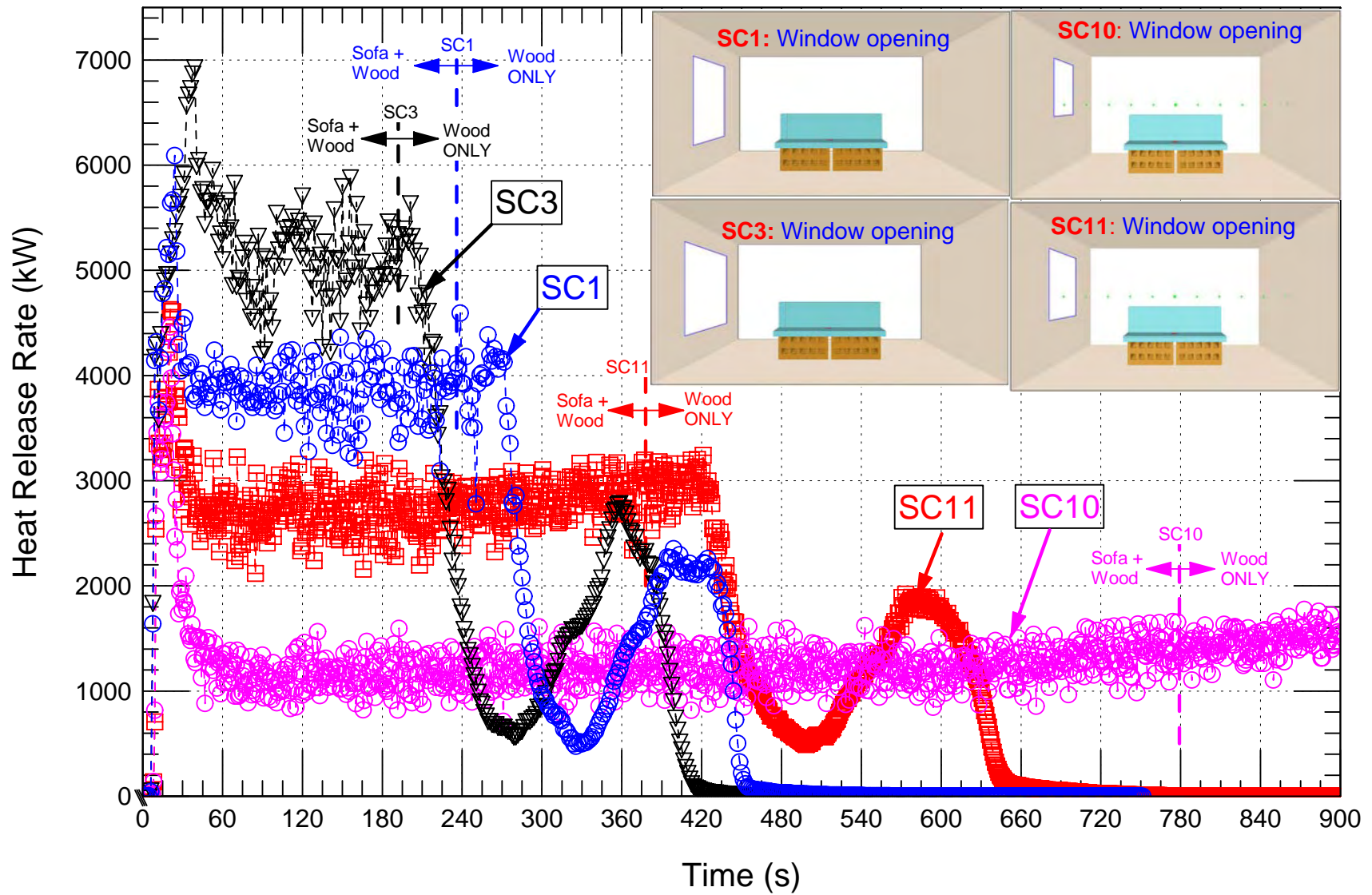


Figure 3-2 Comparison of the HRRs for ventilation scenarios using one window opening with different sizes

## 3.2 Effect of Window Opening Size on Fire Characteristics

In this section, the effect of different sizes of window openings on the fire characteristics is investigated. This includes ventilation scenarios that: (1) use a window opening with different sizes, (2) use a window opening with different sizes and doorway with the same size located in the opposite wall, and (3) use a window opening with different sizes and doorway with the same size located in the same wall.

### Ventilation scenarios using one window opening with different sizes

Figure 3-2 compares the HRRs for SC1, SC3, SC10 and SC11. Scenarios SC1 and SC10 had a square window opening of a size of 1.5 m and 1.0 m, respectively. Scenario SC3 had a large rectangular window opening of a size of 2.0 m wide and 1.5 m high. Additionally, scenario SC11 was considered, which had a rectangular window opening with a size (1.4 m wide and 1.2 m high), which equal the average size of a large number of window openings based on the survey [3]. In these scenarios (Figure 1-2), the fire load was located at the room center, and the coordinates (in meters) of the window opening centers were located at (0.0,1.9,1.25), (0.0,1.9,1.25), (0.0,1.9,1.0) and (0.0,1.9,1.1) for SC1, SC3, SC10 and SC11, respectively (Table 1-1).

As shown in Figure 3-2, the size of the window opening had a significant effect on the fire characteristics during the period of burning in these scenarios. A larger window opening size resulted in higher maximum HRR and a shorter period of burning. For example, the maximum HRR in SC3 with the largest window opening was 6,940 kW compared to 4,400 kW for SC10 with the smallest window opening size (Table 3-1). In all scenarios, after ~60 s from ignition, and during the period of burning the polyurethane sofa and wood cribs simultaneously, and the period of early stage of burning wood only, the HRR was more or less constant.

It took a shorter time for the sofa to be completely burned in scenarios with a larger window opening size. For example, the sofa was completely burned at 192 s in the scenario with the largest window opening size (SC3) compared to 779 s in the scenario with the smallest window opening size (SC10). At these times, the HRRs in SC1, SC3, SC10 and SC11 were ~4,120, 5,350, 1,390, and 2,930 kW, respectively. A snapshot showing the status of the wood cribs at the time when the sofa was completely burned is shown in Figure 3-3 for these scenarios. As shown in this figure, the amount of mass loss from the wood cribs was highest in SC11 (see Table 3-2).

As shown in Figure 3-2, the HRR dropped to its minimum value earlier in the scenario with the larger window opening size. For example, the minimum HRR in scenario SC3 (581 kW at 279 s) was reached 220 s earlier than in scenario SC11 (493 kW at 499 s). Similarly, the second peak of the HRR was reached earlier with a higher value in the scenario with the larger window opening size. For example, the value of the HRR at the second peak in scenario SC3 was 2,800 kW (at 358 s) compared to 2,350 kW (at 399 s) and 1,890 kW (at 583 s) in scenarios SC1 and SC11, respectively. During the period from ~60 s – end of simulation (900 s) in the scenario with the smallest window opening size (SC10), the HRR was more or less constant. The duration of burning in this scenario was the longest (HRR ~1,500 kW at 900s). On the other hand,

the fire was extinguished earlier in the scenario with the larger window opening size. The fire was extinguished (HRR ~ 1 kW) after 545, 600, and 823 s in SC3 (2.0x1.5 m window opening), SC1 (1.5x1.5 m window opening), and SC11 (1.4x1.2 m window opening), respectively. Snapshots showing the status of the wood cribs at the time when the fire was extinguished in scenarios SC1, SC3 and SC11, and at the end of simulation (900 s) are shown in Figure 3-4. As shown in this figure, the amount of mass loss was the highest in scenario SC11 (see Table 3-3).

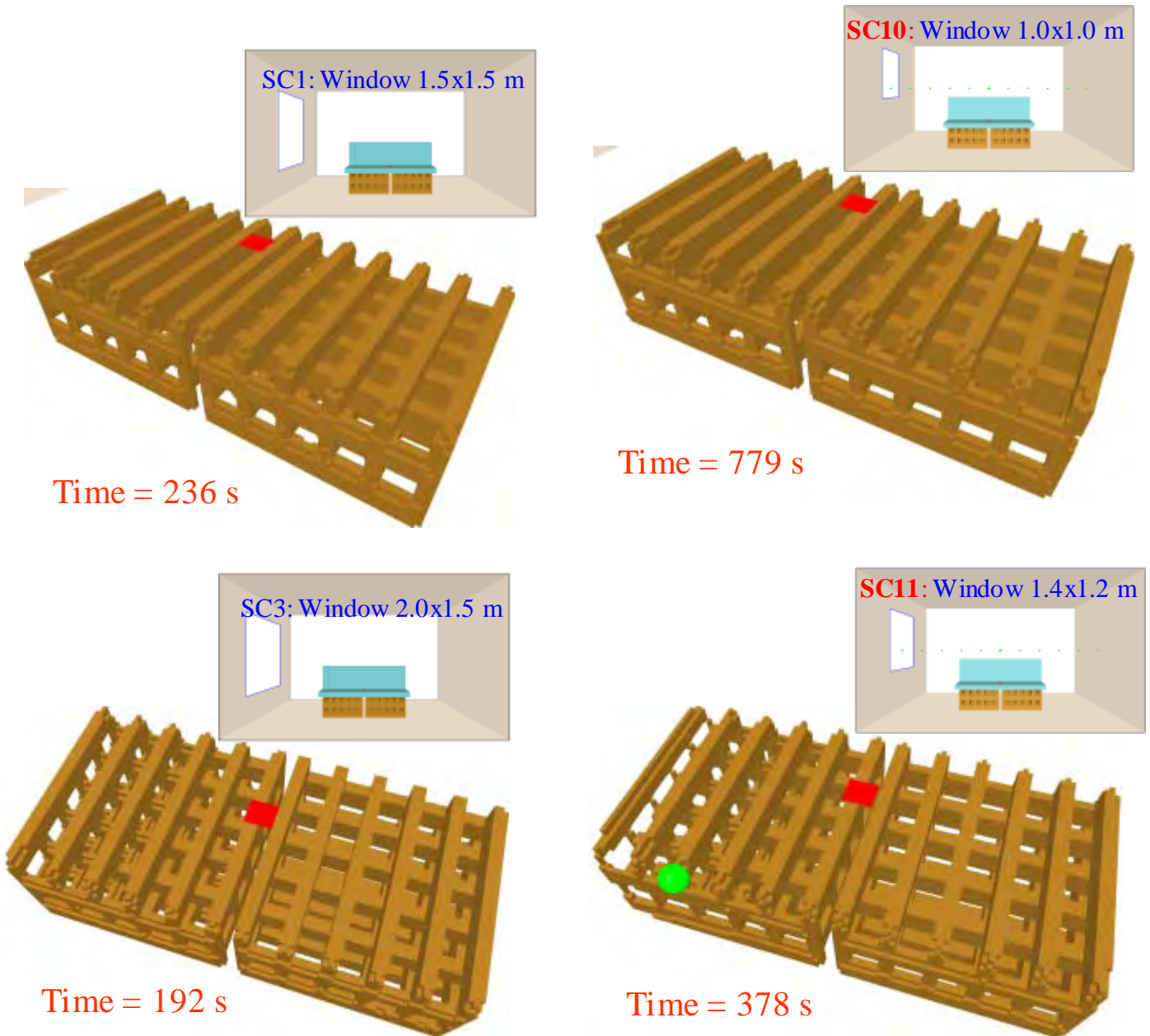


Figure 3-3 Status of the wood cribs at the time at which the polyurethane sofa was completely burned in SC1, SC3, SC10 and SC11

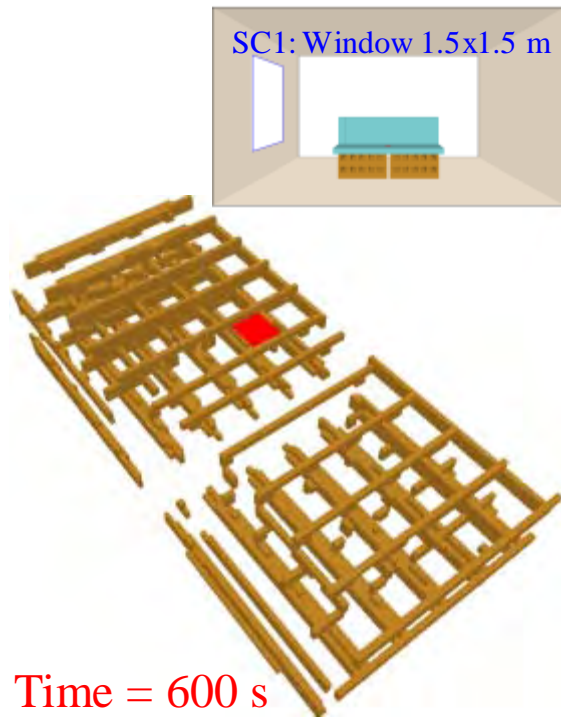


Figure 3-4 Status of the wood cribs when the burning stopped in SC1, SC3 & SC11 (HRR = ~1 kW) and at the end of simulation in SC10 (HRR ~ 1500 kW at 900 s)

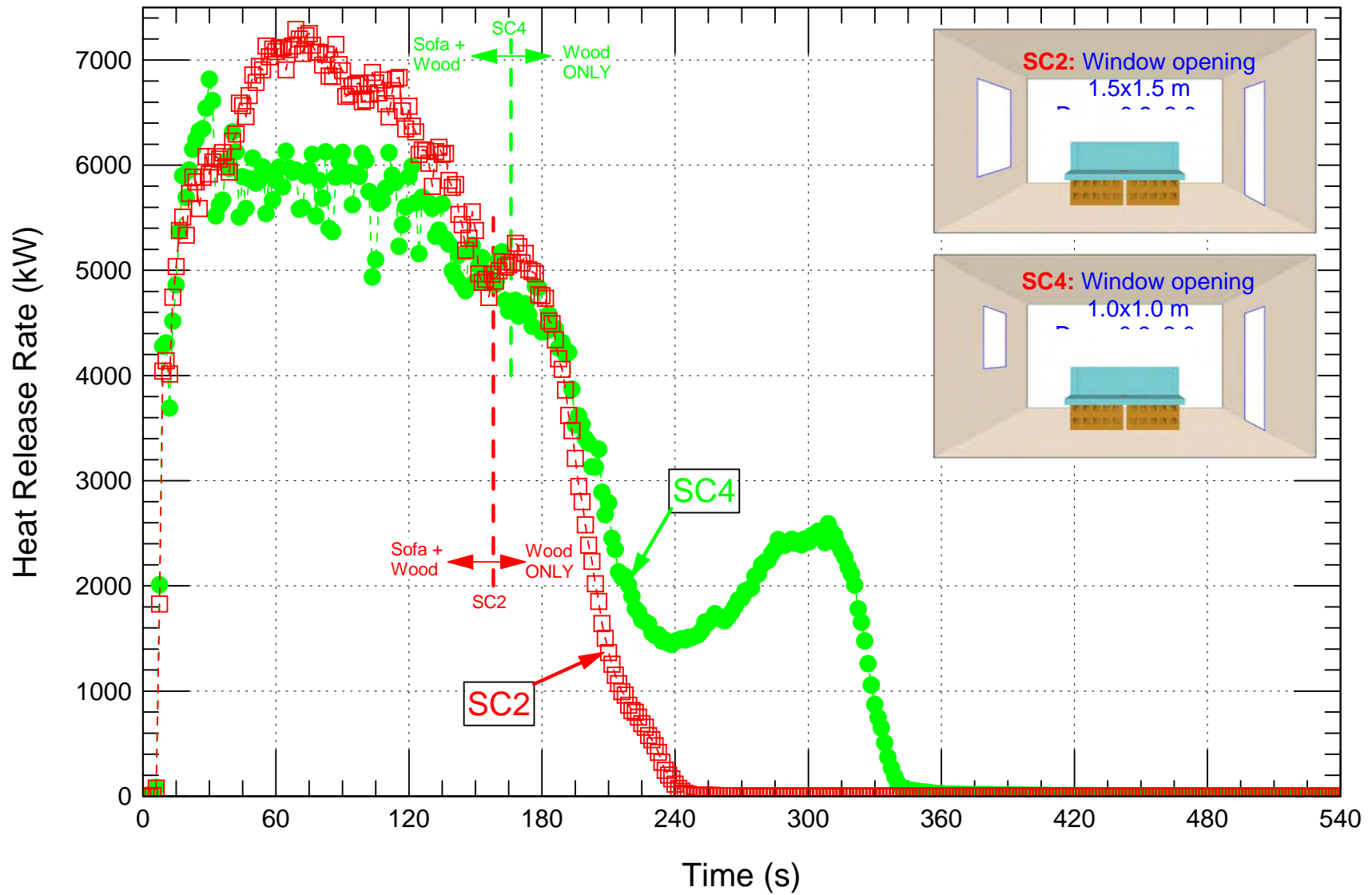


Figure 3-5 Comparison of the HRRs for ventilation scenarios using window opening (different sizes) and doorway (same size) facing each other

## Ventilation scenarios using a window opening and doorway in the opposite walls

Figure 3-5 compares the HRR for SC2 and SC4. Scenarios SC2 and SC4 had a square window opening of a size of 1.5 m and 1.0 m, respectively. The coordinates (in meters) of the center of the window openings were (0.0, 1.9, 1.25) and (0.0, 1.9, 1.5) for SC2 and SC4, respectively. Both scenarios had a rectangular opening of a size of 0.9 m wide and 2.0 m high located in the wall opposite the window opening and its center was located at (4.2, 1.9, 1.0) (Table 1-1). The fire load was located at the room center in both scenarios (Figure 1-3).

Figure 3-5 clearly showed that the HRRs in these scenarios were different. The scenario with a larger window opening size (SC2) resulted in a higher maximum HRR (7,292 kW in SC2 compared to 6,816 kW in SC4). The HRR at its second peak in the scenario with the larger window opening size (SC2) was much higher (5,258 kW) and reached 141 s earlier (at 168 s) than that in the scenario with the smaller window opening size (SC4) (2,591 kW at 309 s). The minimum HRR before reaching its second peak in SC2 (4,744 kW occurred at time = 156 s) was also much higher than that in SC4 (1,442 kW occurred at time = 238 s).

Figure 3-6 shows a snapshot of the status of the wood cribs when the sofa was completely burned. In these two scenarios, the sofa took about the same time to be completely burned (158 s and 166 s in SC2 and SC4, respectively). Also, at this time, the amount of mass loss from the wood was slightly larger in the scenario with the larger window opening size (49.0 kg in SC2 compared to 48.3 kg in SC4, Table 3-2).

The size of the openings and their locations play an important role in the thermal feedback to the bulk fuel and its surface temperature, and hence on the fire development. Because of the larger amount of heat losses by convection and radiation through the openings in the scenario with the larger window opening size (SC2), the amount of net heat feedback to the fuel surface was smaller. As a result, the fire lasted for a shorter period in the scenario with the larger window opening size (300 s in SC2 compared to 435 s in SC4). Figure 3-7 shows a snapshot of the status of the wood cribs when the fire was extinguished (HRR ~ 1 kW). As shown in this figure, scenario SC4 resulted in more mass loss than scenario SC2. The remaining mass from the wood cribs in scenario SC2 was 31% compared to 21% (by mass) in scenario SC4 (Table 3-3).

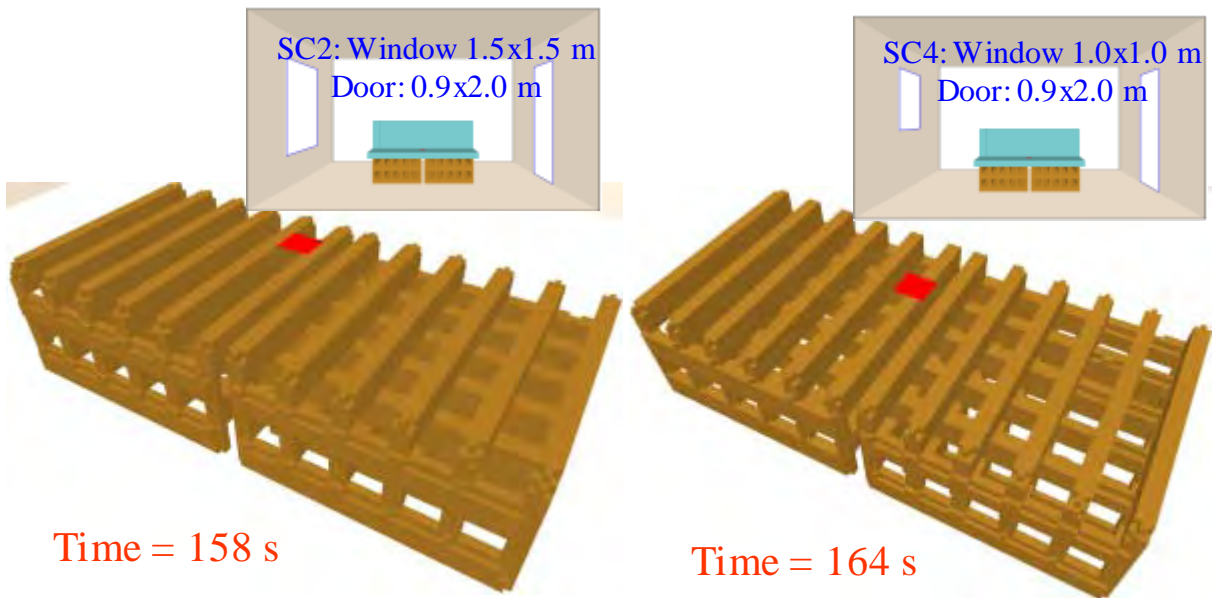


Figure 3-6 Status of the wood cribs at time at which the polyurethane sofa was completely burned in SC2 and SC4

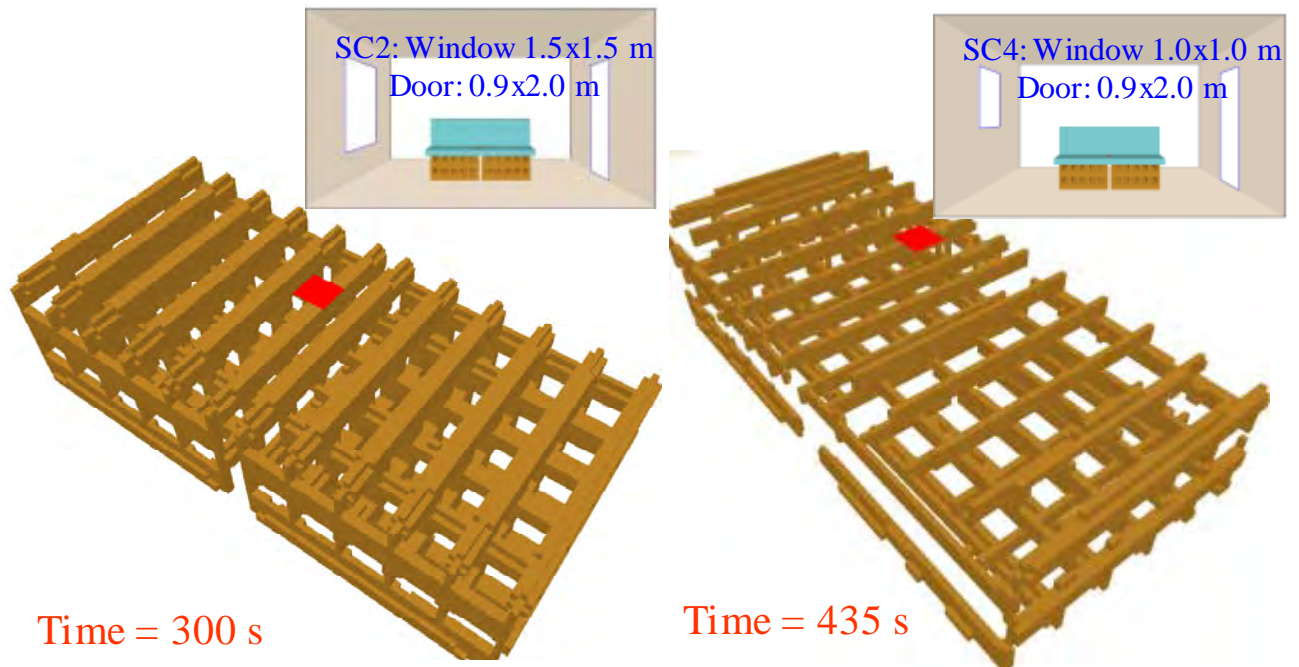


Figure 3-7 Status of the wood cribs when the burning stopped in SC2 and SC4 (HRR = ~1 kW)

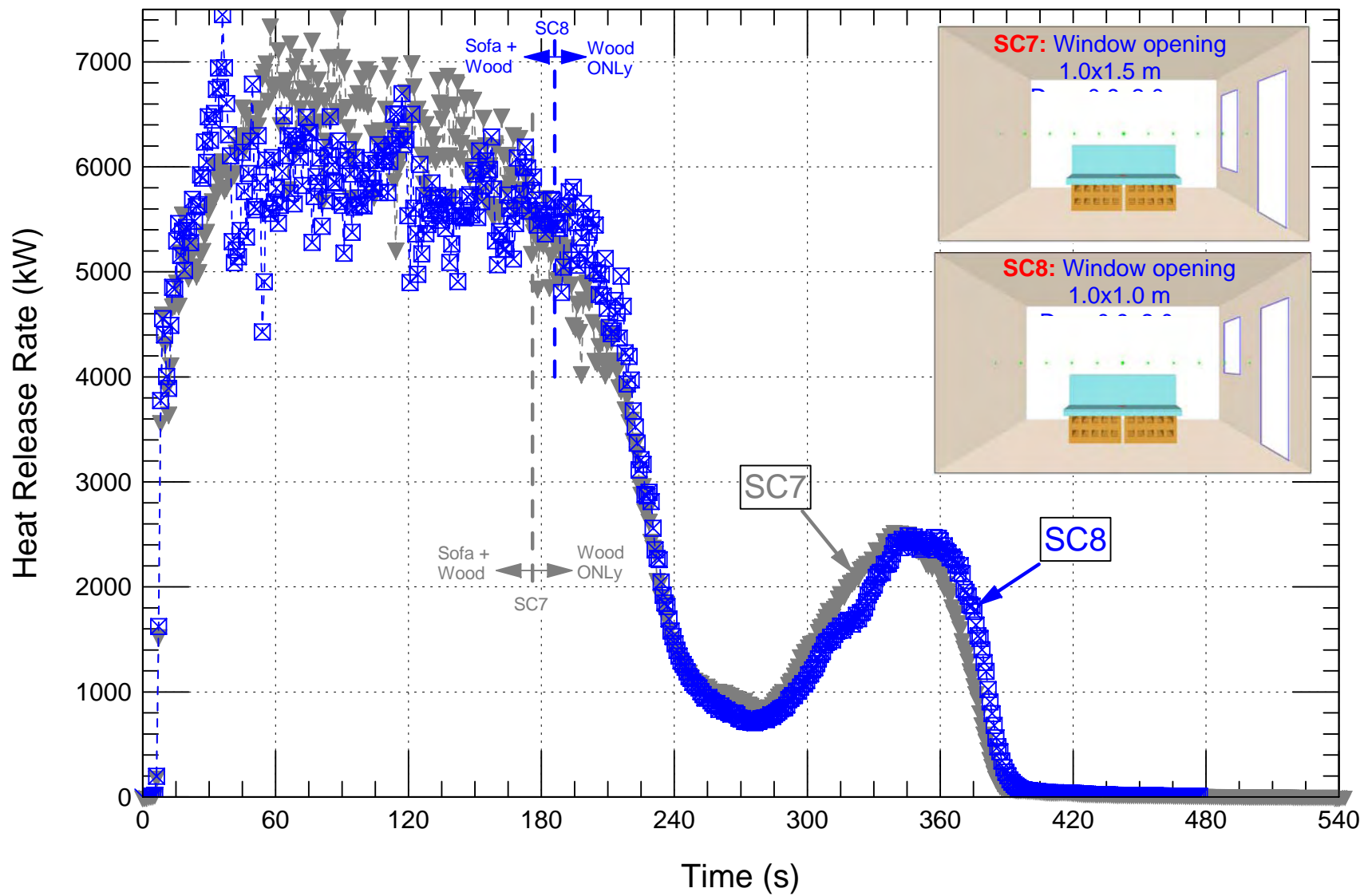


Figure 3-8 Comparison of the HRRs for ventilation scenarios using window opening (different sizes) and doorway (same size) located in the same wall side

## Ventilation scenarios using a window opening and doorway in the same wall

Figure 3-8 compares the HRR when both the window opening and doorway were located on the same wall in scenarios SC7 and SC8. Scenario SC7 had a rectangular window opening of a size of 1.0 m wide and 1.5 m high, while SC8 had a window opening of a square exterior opening of a size of 1.0 m (Figure 1-4). The coordinates (in meters) of the window opening centers were (4.2,2.85,1.25) and (4.2,2.85,1.5) in SC7 and SC8, respectively (Table 1-1). A doorway of a rectangular exterior opening of a size of 0.9 m wide and 2.0 m high was used in both scenarios. As shown in Figure 3-8, there was insignificant difference in the fire characteristics during the whole period of burning in these scenarios. For example, the maximum HRRs were about the same in both scenarios (7,431 kW and 7,450 kW in SC7 and SC8, respectively). The sofa was completely burned at 176 s and 186 s in SC7 and SC8, respectively (Table 3-2 and Figure 3-9). Additionally, the remaining mass from the wood cribs was the same in both scenarios (20% by mass) (Table 3-3 and Figure 3-10). More details about the flow field in the room, locations of the neural planes in the window opening and doorway, etc. are available in [1].

In summary, in the case of using a window opening and doorway in the same wall, the size of the window opening did not affect the fire characteristics (see SC7 and SC8). However, the size of the window opening had a significant effect on the fire characteristics in the cases of using a window opening and doorway in opposing walls (see SC2 and SC4), and only a window opening (see SC1, SC3, SC10 and SC11).

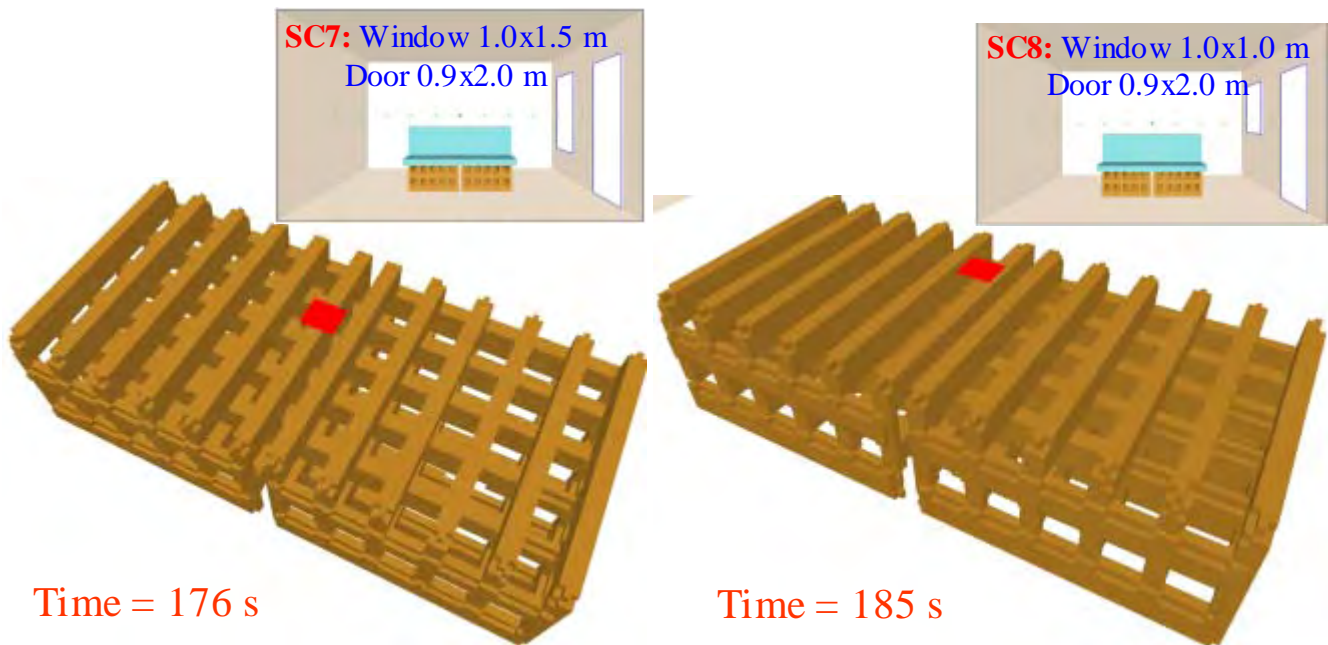


Figure 3-9 Status of the wood cribs at time at which the polyurethane sofa was completely burned in SC7 and SC8

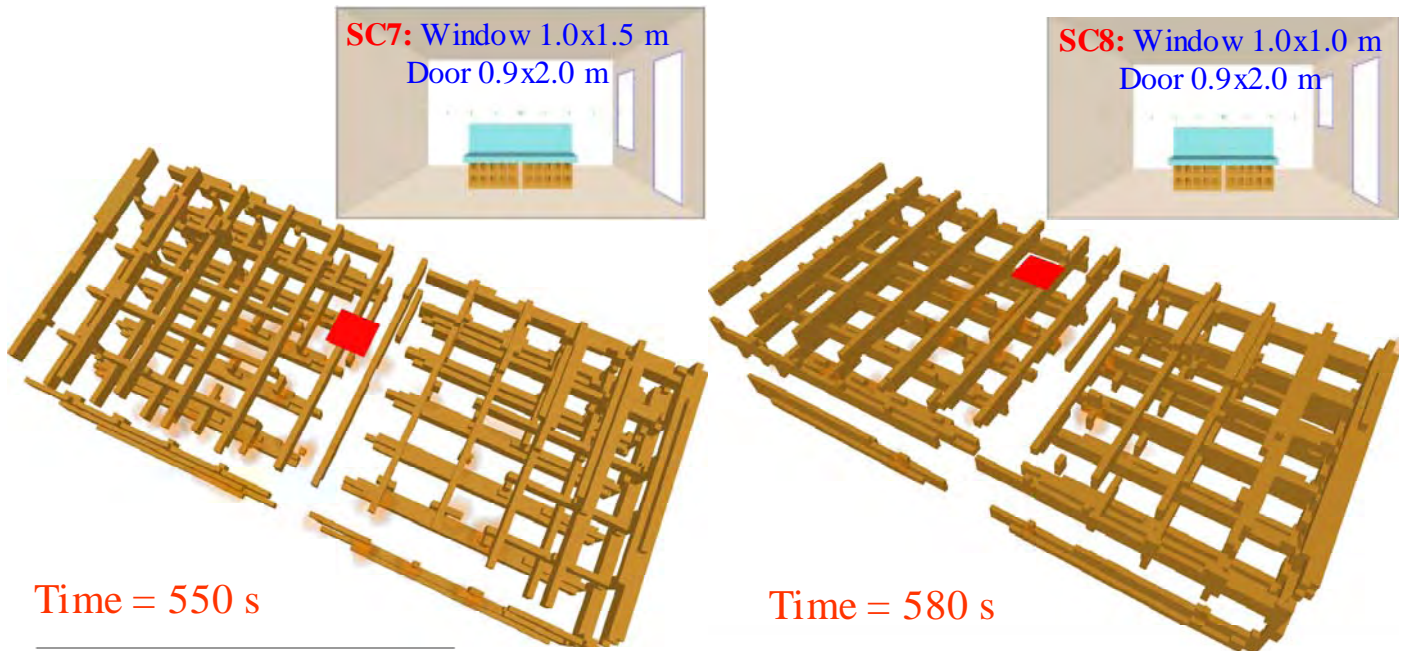


Figure 3-10 Status of the wood cribs when the burning stopped in SC7 and SC8 (HRR = ~1 kW)

### 3.3 Effect of Doorway Size on Fire Characteristics

The ventilation scenario SC6 was similar to scenario SC5 except for having a wider doorway of a size of 1.5 m wide and 2.0 m high in the former compared to 0.9 m wide and 2.0 m high in the latter. The coordinates (in meters) of the doorway center in both scenarios were (4.2, 1.9, 1.0) (Table 1-1). The fire load was located at the room center in both scenarios (Figure 1-5).

Figure 3-11 compares the HRR for scenarios SC5 and SC6. As shown in this figure, the doorway size had a significant effect on the HRR. In the first 15 s, the HRR increased rapidly in both scenarios. After that the HRR increased further but with a lower rate and reached its first peak (7,069 kW) at 85 s in the scenario with a larger doorway size (SC6). In scenario SC5, however, the first peak HRR (4,983 kW) was achieved after ~15 s from initiating the fire, and within 12 s after reaching the first peak (from 15 s to 27 s), the HRR decreased rapidly with time from 4,983 kW to 3,460 kW.

As shown in Figure 3-11, the minimum HRR before reaching its second peak in the scenario with a larger doorway size (SC6) was much higher (4,156 kW) and reached 152 s earlier (at 167 s) than for scenario SC5 with a smaller doorway size (1,521 kW at 319 s). Furthermore, the value of the HRR at its second peak in SC6 was much higher (4,513 kW) and reached 171 s earlier (at 180 s) than for scenario SC5 (1,961 kW at 351 s). The sofa was completely burned in scenario SC6 at 167 s versus 249 s in scenario SC5. At these times, the amount of mass loss from the wood in the scenario with a smaller doorway size (SC5) was 52.4 kg (60% by mass) compared to 47.1 kg (54% by mass) in scenario SC6 (see Figure 3-12 and Table 3-2).

The larger exterior opening in SC6 (1.5 m x 2.0 m doorway) resulted in more heat losses (by convection and radiation) than that in SC5 (0.9 m x 2.0 m doorway). As such, the net thermal feedback to the fuel in SC6 was lower than that in SC5. For this reason, it took a shorter period to completely extinguish the fire in SC6 (346 s) than that in SC5 (536 s). A snapshot for the status of the wood when the fire was extinguished (HRR ~ 1 kW) is shown in Figure 3-13. At these times, the unburned mass of the wood was 25.6 kg (29% by mass) in SC6 compared to 18.3 kg (21% by mass) in SC5 (Table 3-3).

In the scenario with a larger doorway size (SC6), the total energy released due to burning 69.5 kg of the fire load (61.2 kg wood and 8.3 kg polyurethane sofa) was 1,198 MJ. The total energy released in this scenario (SC6) was about the same as in scenario SC5 (1,219 MJ), although the total mass loss in the former (69.5 kg) was 7.2 kg smaller than that in the latter (76.7 kg). Having a larger doorway size in scenario SC6 than in scenario SC5 resulted in higher oxygen concentration inside the compartment in the former than in the latter. Accordingly, the amount of CO production in the former was smaller (due to converting most of the CO to CO<sub>2</sub>) than in the latter. As a result, the effective heat of combustion in scenario SC6 (17.2 MJ/kg) was greater than that in scenario SC5 (15.9 MJ/kg) (see Table 3-3). More details about the flow field in the room, locations of the neutral plane in the doorways, etc are available in [1].

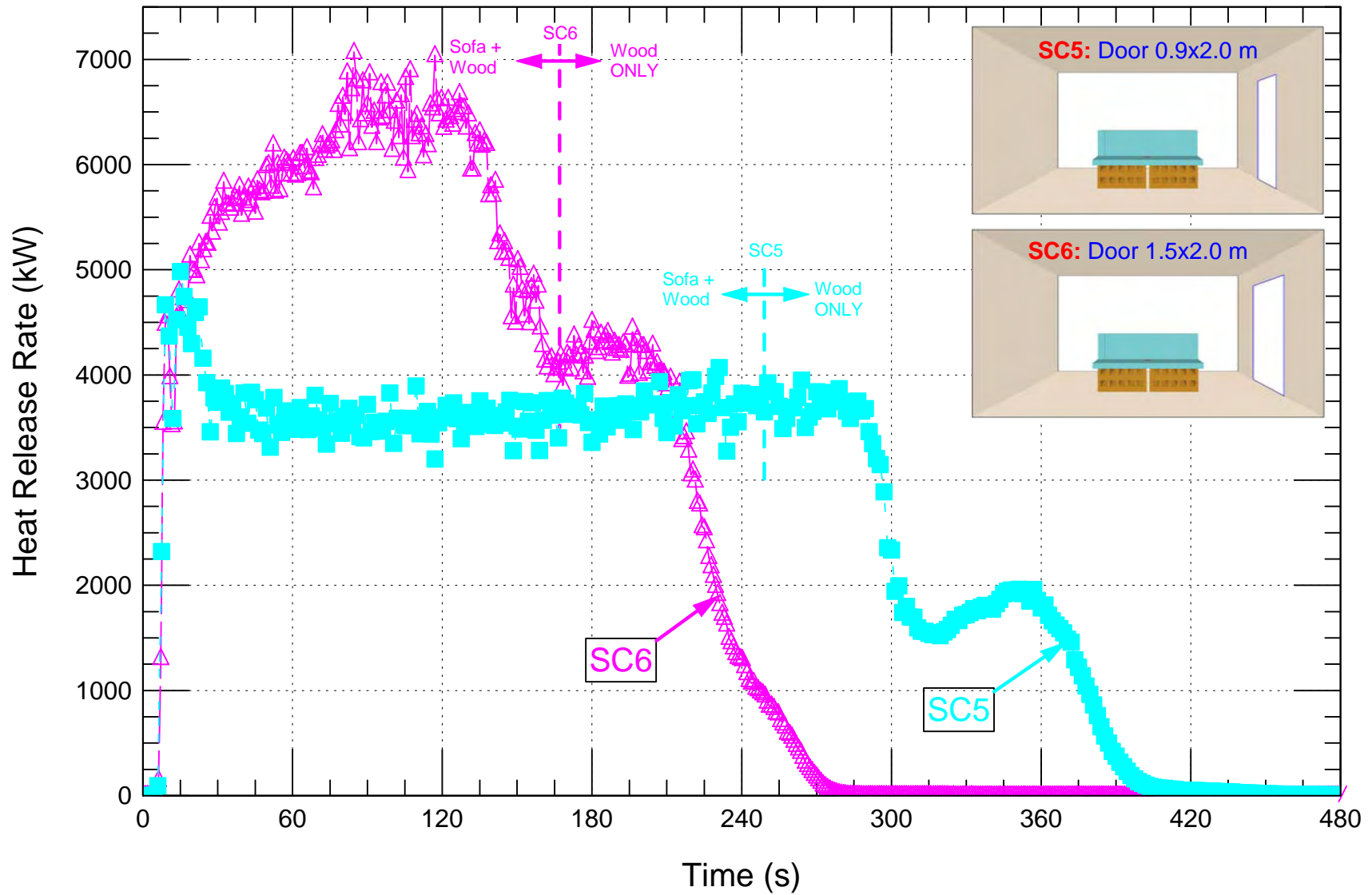


Figure 3-11 Comparison of the HRRs for ventilation scenarios using a doorway with different sizes

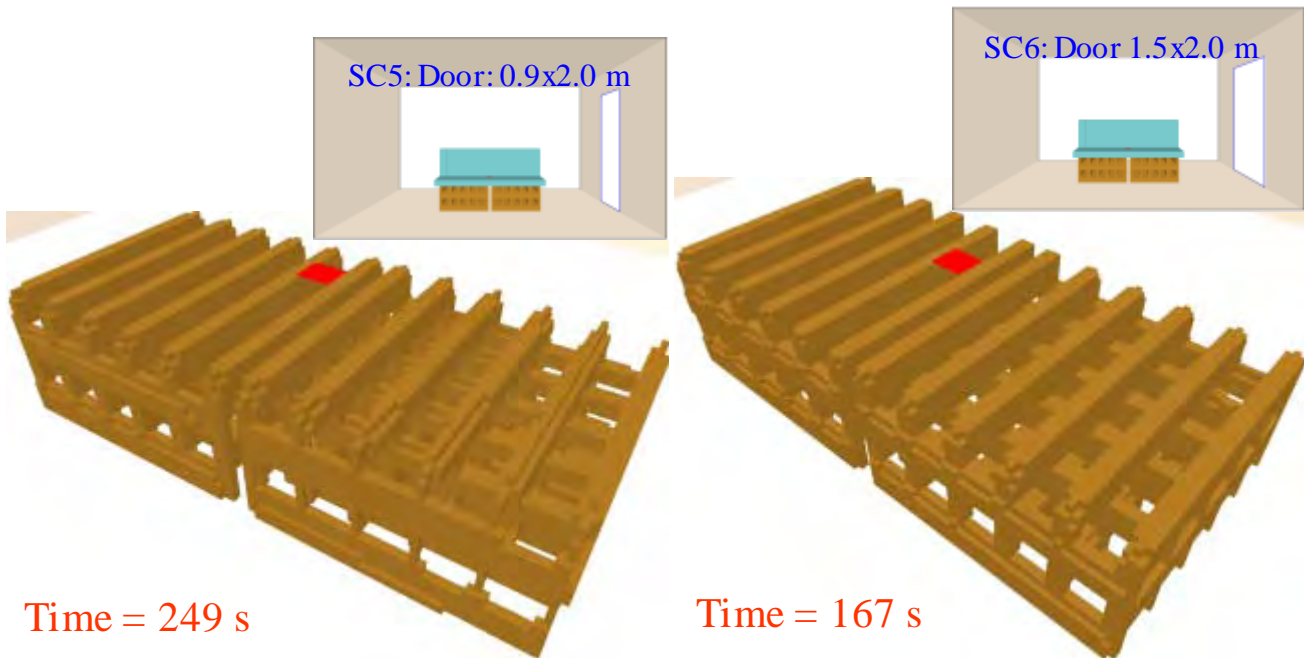


Figure 3-12 Status of the wood cribs at time at which the polyurethane sofa was completely burned in SC5 and SC6

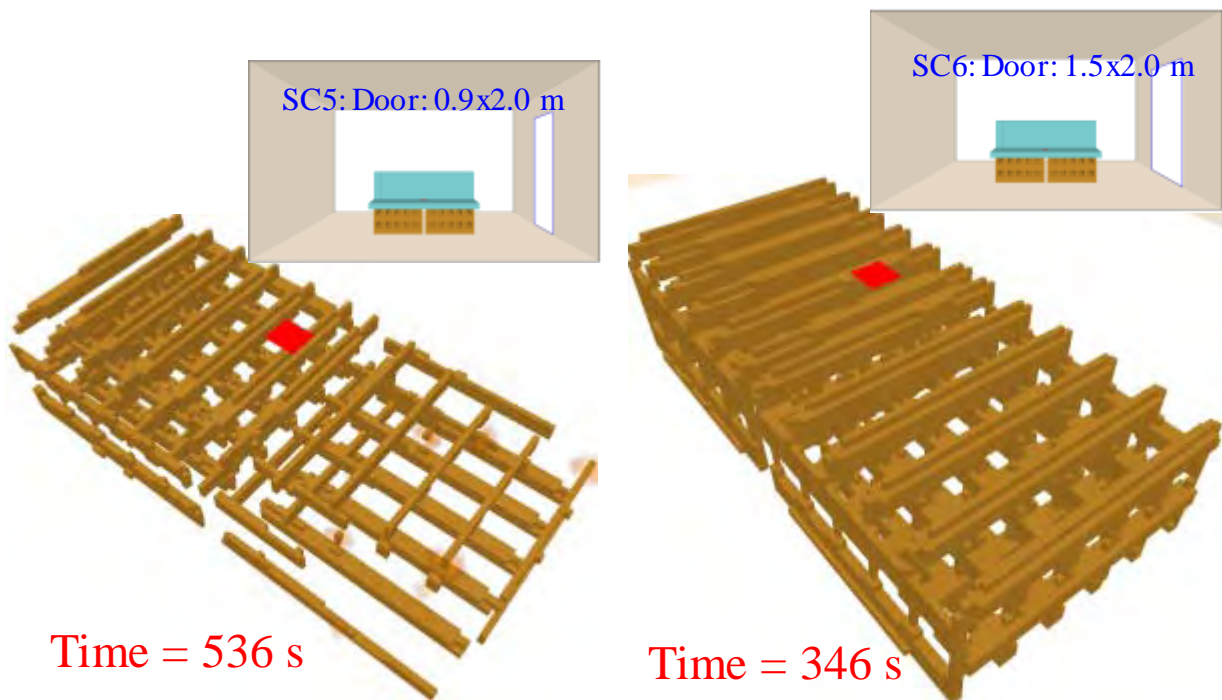


Figure 3-13 Status of the wood cribs when the burning stopped in SC5 and SC6 (HRR = ~1 kW)

### 3.4 Effect of Fire Location on Fire Characteristics

The ventilation scenario SC9 is similar to scenario SC3 except for placing the fire load at the northeast corner of the room in the former (100 mm from both the east and north walls), and at the room center in the latter (Figure 1-6). A rectangular window opening of a size of 2.0 m wide and 1.5 m high was used in these two scenarios. The coordinates (in meters) of the center of the window opening were (0.0,1.9,1.25) (Table 1-1). In SC9, a square exterior opening of a size of 0.2 m represented the leakage in the room and the coordinates of its center were (4.2,3.3,0.2).

Figure 3-14 shows the HRR for scenarios SC3 and SC9. As shown in this figure, the maximum HRR in scenario SC3 was much higher (6,940 kW) and reached much earlier (at 39 s) than in scenario SC9 (4,760 kW at 282 s). The sofa took a longer period to be completely burned in SC9 (283 s) than in scenario SC3 (192 s). Figure 3-15 shows a snapshot for the status of the wood cribs at the time when the sofa was completely burned in these scenarios. At this time, the mass loss from the wood cribs in scenario SC9 (53.4 kg, 62% by mass) was higher than in scenario SC3 (49.0 kg, 57% by mass). In both scenarios, after the sofa was completely burned, the HRR decreased and reached a minimum value of 581 kW at 279 s, and 594 kW at 375 s in SC3 and SC9, respectively. The second peak of the HRR in scenario SC3 was higher (2,800 kW) and reached 87 s earlier than in scenario SC9 (1,740 kW at 445 s).

Because the fire load was closer to the window opening in scenario SC3, the amount of heat losses by convection and radiation through it was higher than that in scenario SC9. Consequently, the amount of net heat feedback to the surface of the fuel was lower in SC3 than that in SC9. As a result, the duration of burning was 100 s shorter in scenario SC3 (545 s) than in scenario SC9 (645 s). A snapshot of the status of the wood when the fire was extinguished (HRR ~ 1 kW) is shown in Figure 3-16 for these scenarios. As shown in this figure, the amount of mass loss in scenario SC9 was greater than in scenario SC3. In summary, the fire load location had a significant effect on the fire characteristics.

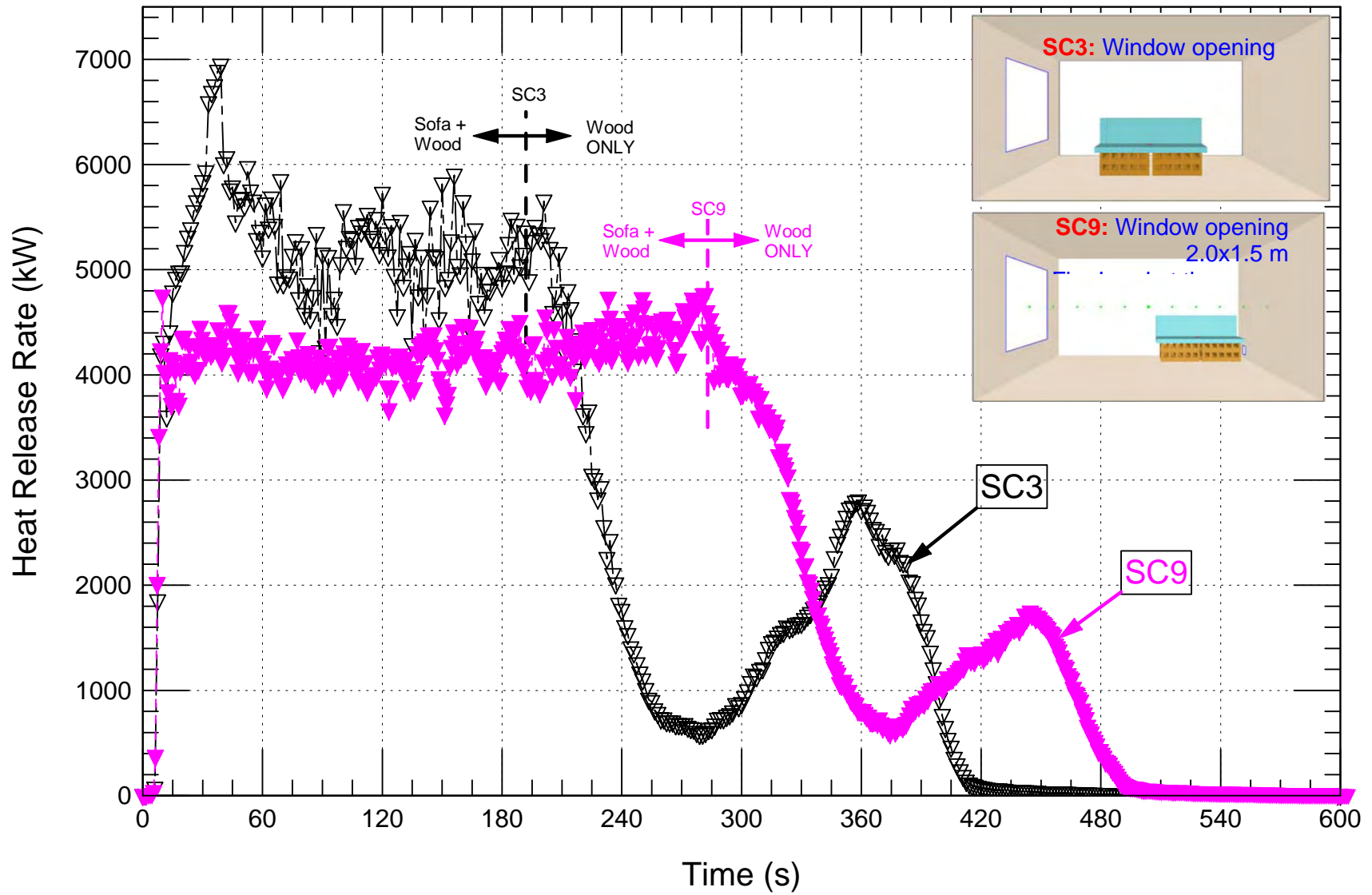


Figure 3-14 Comparison of the HRRs for ventilation scenarios using same window opening size and different fire load locations

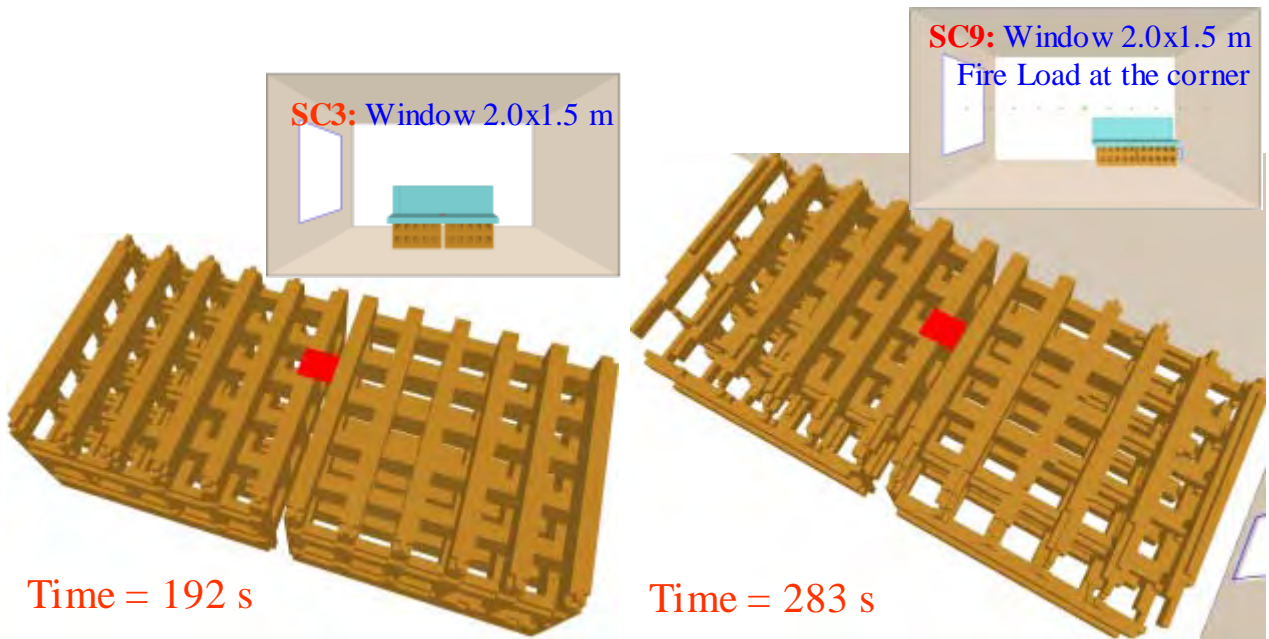


Figure 3-15 Status of the wood cribs at time at which the polyurethane sofa was completely burned in SC3 and SC9

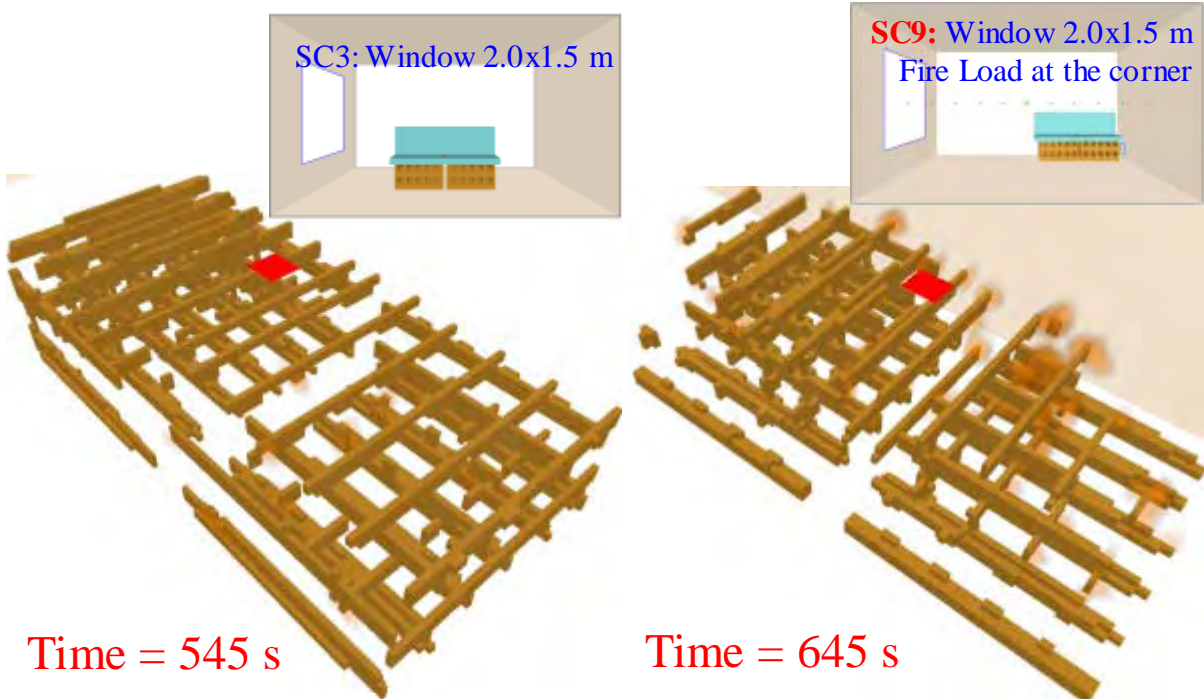


Figure 3-16 Status of the wood cribs when the burning stopped in SC3 and SC9 (HRR = ~1 kW)

Table 3-1 Comparison of the maximum HRR and burning rate of all scenarios

Ventilation Scenario	Maximum Heat Release Rate and its Time		Maximum Burn Rate and its Time	
	kW	s	kg/s	s
<b>SC1</b>	6,092	24	0.405	59
<b>SC2</b>	7,292	69	0.517	66
<b>SC3</b>	6,940	39	0.508	113
<b>SC4</b>	6,816	30	0.531	59
<b>SC5</b>	4,983	15	0.347	72
<b>SC6</b>	7,069	85	0.495	87
<b>SC7</b>	7,431	88	0.513	57
<b>SC8</b>	7,450	36	0.495	54
<b>SC9</b>	4,760	282	0.324	186
<b>SC10</b>	4,400	21	0.267	21
<b>SC11</b>	4,620	23	0.257	21

Table 3-2 Comparison of the time and burned mass when sofa completely burned

Ventilation Scenario	Time at which the sofa was completely burned, t* (s)	Burned mass of the wood cribs at t* (kg)	Total burned mass at t* (kg)	Percentage of Wood Cribs Burned at t* (%w)
SC1	236	50.6	58.9	58
SC2	158	49.0	57.3	57
SC3	192	49.6	57.9	57
SC4	166	48.3	56.6	56
SC5	249	52.4	60.7	60
SC6	167	47.1	55.4	54
SC7	176	47.2	55.5	54
SC8	186	48.4	56.7	56
SC9	283	53.4	61.7	62
SC10	779	46.3	54.3	53
SC11	378	50.9	59.2	59

Table 3-3 Comparison of the total mass losses, total energy release and the effective heat of combustion

Ventilation Scenario	Total burned mass of the wood cribs (kg)	Total burned mass (sofa + wood cribs) (kg)	Total remaining mass of the wood cribs (kg)	Percentage of total remaining mass of the wood cribs (%w)	Total Energy released (MJ)	Effective Heat of Combustion (MJ/kg)
SC1	70.9	79.1	15.9	18	1,317	16.6
SC2	59.7	68.0	27.0	31	1,169	17.2
SC3	69.9	78.2	16.8	19	1,398	17.9
SC4	68.8	77.1	17.9	21	1,304	16.9
SC5	68.4	76.7	18.3	21	1,219	15.9
SC6	61.2	69.5	25.6	29	1,198	17.2
SC7	69.6	77.9	17.1	20	1,515	19.4
SC8	69.3	77.6	17.4	20	1470	18.9
SC9	69.5	77.8	17.2	20	1,511	19.4
SC10 <sup>#</sup>	56.5	64.8	30.2	35	1,159	17.9
SC11	71.5	79.8	15.2	18	1,449	18.2

<sup>#</sup> Burning was still going with a heat release rate of ~1,500 kW at the end of simulation (900 s)

### 3.5 Stage of Fully-Developed Fire (Post-flashover)

Fully-developed (post-flashover) fire scenarios are typically used in the design and analysis of building fire safety systems, such as structural fire resistance or in estimating the potential for building-to-building fire spread. The stage of post-flashover is defined as the period when the mass of fuel was between 80% and 30% of the original, unburned fuel mass [8]. There are several models and correlations available to predict the temperature of fully-developed enclosure fires [8 –11]. These models and correlations predict compartment fire temperature based on input data for heat release curves, the amount of fuel in the compartment and compartment characteristics (e.g. compartment geometry, ventilation setting, and thermal properties of construction materials). While much attention has been focused on computer modelling in recent years, closed-form models are still representative of the state of the art in post-flashover enclosure fire modelling.

Recently Hurley [8] evaluated the closed-form models of fully-developed enclosure fires by comparing predictions of different correlations with temperature data from experiments. The selected experimental data represented a wide spectrum of ventilation conditions, including fuel- and ventilation-controlled fires. Most of the available correlations were found to under-predict compartment fire temperatures under some conditions [8].

In this section, the average temperature within the compartment and burning rate or the fuel mass losses during the stage of post-flashover were investigated for all ventilation scenarios. Additionally, the temperatures averaged over the period of post-flashover based on CFD simulations for all scenarios (SC1 through SC11) are presented as a function of ventilation factor,  $\Psi$  ( $\Psi = A_o \sqrt{H_o} / A_T$ ). These temperatures were compared with that obtained using Babrauskas' correlation [11].

#### Babrauskas' correlation for post-flashover

The average gas temperature in post-flashover based on the work of Babrauskas [11] is given as:

$$T_g = T_\infty + (T^* - T_\infty) \times \theta_1 \times \theta_2 \times \theta_3 \times \theta_4 \times \theta_5, \quad (3-1)$$

where:

$T_g$  = average gas temperature (K)

$T_\infty$  = ambient temperature (K)

$T^*$  = empirical constant = 1725 K

The factors  $\theta_1$  through  $\theta_5$  in the above equation account for different physical phenomena, which are burning rate stoichiometry ( $\theta_1$ ), wall steady-state heat losses ( $\theta_2$ ), wall transient heat losses ( $\theta_3$ ), opening height effect ( $\theta_4$ ), and combustion efficiency ( $\theta_5$ ). These factors are listed below:

$$\theta_1 = \begin{cases} 1.0 + 0.51 \ln \phi & \text{for } \phi < 1 \\ 1.0 - 0.05 (\ln \phi)^{5/3} & \text{for } \phi > 1 \end{cases}, \phi = \frac{HRR}{1500 A_o \sqrt{H_o}}, \quad (3-2)$$

$$\theta_2 = 1.0 - 0.94 \exp \left[ -54 \left( \frac{A_o \sqrt{H_o}}{A_T} \right)^{2/3} \left( \frac{\delta}{k} \right)^{1/3} \right], \quad (3-3)$$

$$\theta_3 = 1.0 - 0.92 \exp \left[ -150 \left( \frac{A_o \sqrt{H_o}}{A_T} \right)^{0.6} \left( \frac{t}{k \rho C_p} \right)^{0.4} \right], \quad (3-4)$$

$$\theta_4 = 1.0 - 0.205 H_o^{-0.3}, \text{ and} \quad (3-5)$$

$$\theta_5 = 1.0 + \ln b_p. \quad (3-6)$$

Where,

$HRR$  = heat release rate (kW),

$A_o$  = area of the opening(s) ( $m^2$ ),

$A_T$  = total area of the compartment – enclosing surfaces ( $m^2$ ),

$b_p$  = the combustion efficiency with values in the range 0.5 – 0.9,

$C_p$  = wall specific heat (J/kg.K),

$H_o$  = height of the opening (m),

$k$  = wall thermal conductivity (W/m.K),

$t$  = time (s),

$\delta$  = wall thickness (m),

$\rho$  = wall density ( $kg/m^3$ ), and

$\phi$  = equivalence ratio ( $\phi = 1$  at stoichiometry,  $\phi > 1$  for fuel-rich burning, and  $\phi < 1$  for fuel-lean conditions).

Note that in the case of having more than one opening such as in scenarios SC2, SC4, SC7 and SC8, the height of the opening ( $H_o$ ) is calculated as the weighted average of the height as following:

$$H_o = \frac{\sum_{i=1}^n A_{o,i} H_{o,i}}{\sum_{i=1}^n A_{o,i}}, \quad (3-7)$$

where,

$n$  = number of openings.

Figure 3-17 and Table 3-4 compare the predicted temperature averaged over the period of post-flashover based on the CFD simulations and that obtained using Babrauskas' correlation [11]. As mentioned earlier, the walls and ceiling of the compartment were insulated in the CFD simulations, which represented the most severe condition. On the other hand, some of the empirical constants in the Babrauskas' correlation [11] were obtained based on the experimental data (i.e. heat losses through the walls and ceiling were accounted for). As such, the present CFD predictions for the average

temperatures of different ventilation scenarios were higher ( $\leq +25\%$ ) than that obtained using Babrauskas' correlation [11] (see Figure 3-17).

Table 3-4 Calculated average temperature over the period of post-flashover based on CFD simulations and Babrauskas' correlation [11] for all scenarios

Ventilation Scenario	Total Opening Area (m <sup>2</sup> )	Average Temperature based on CFD Simulations (°C)	Average Temperature based on Babrauskas' Correlation [11] (°C)
SC1	2.25	740	694
SC2	4.05	579	545
SC3	3	885	739
SC4	2.8	896	721
SC5	1.8	836	685
SC6	3	852	761
SC7	3.3	923	790
SC8	2.8	903	773
SC9	3	715	737
SC10	1	577	459
SC11	1.68	675	620

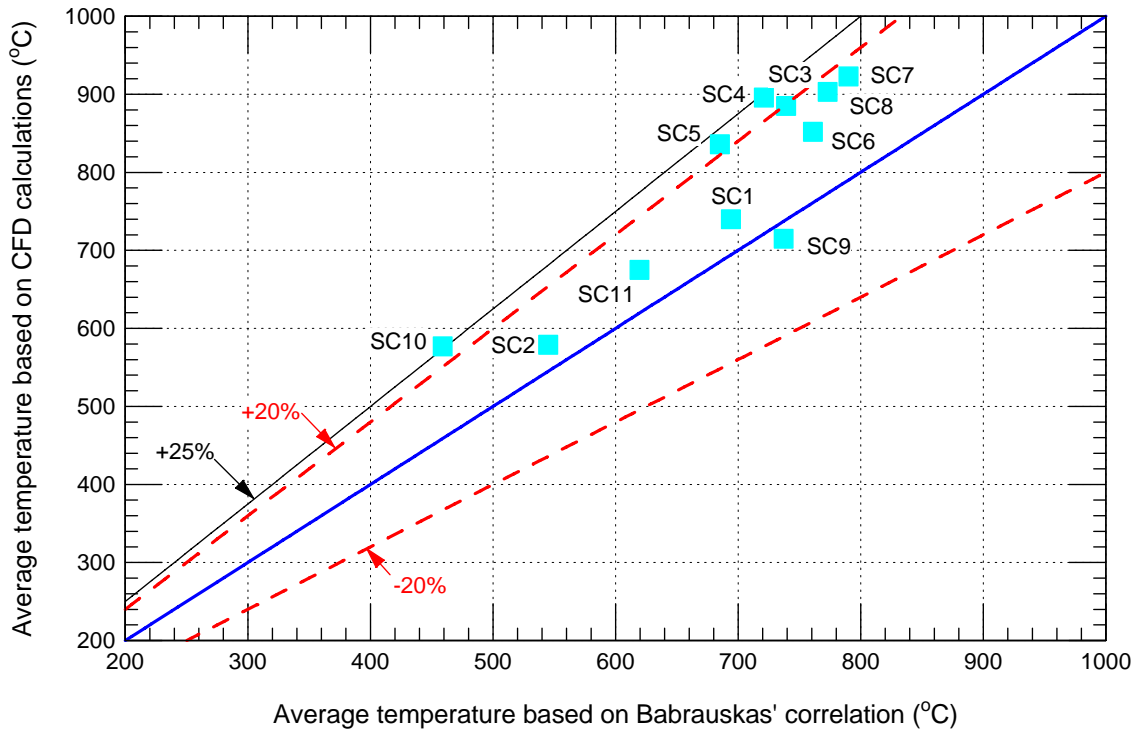


Figure 3-17 Comparison of the average temperature over the period of post-flashover with that obtained using Babrauskas' correlation [11] for all scenarios

## Temperature and mass loss during post-flashover stage

In this subsection, the average compartment temperature and mass loss are compared for each set of ventilation scenarios during the stage of fully-developed fire (post-flashover). As mentioned earlier, the stage of post-flashover was defined as the period when the mass of fuel was between 80% and 30% of the original, unburned fuel mass [8]. Predicting both the temperature and the onset of post-flashover and its period are important in terms of fire spread, and structure integrity and its fire resistance point of view. Figure 6-1 through Figure 6-11 in Appendix – A, show the average temperature and mass loss for each ventilation scenario (SC1 through SC11).

Figure 3-18 compares the temporal change of the average temperature within the compartment and mass loss for ventilation scenarios using only a window opening with different sizes. As shown in this figure, the average temperature increased by increasing the window opening size. The calculated temperature averaged over the period of post-flashover in scenarios SC3 (2.0x1.5 m window opening, largest size), SC1 (1.5x1.5 m window opening), SC11 (1.4x1.2 m window opening) and SC10 (1.0x1.0 m window opening, smallest size) were 885, 740, 675 and 577°C, respectively. As shown in Figure 3-18, the onset of post-flashover took place earlier for ventilation scenarios with a larger window opening size. For example, in scenarios SC3, SC1, SC11 and SC10, the onset of post-flashover occurred at 65, 100, 132 and 304 s, respectively. Furthermore, the period of the post-flashover decreased by increasing the window opening size. These periods were 174 s (from 65 – 239 s), 254 s (from 100 – 354 s), 291 s (from 132 – 423 s), and ~600 s (from 304 – ~900 s, see Figure 6-10 in Appendix – A for the entire range of the period of post-flashover) in scenarios SC3, SC1, SC11 and SC10, respectively.

Figure 3-19 compares the average temperature and mass loss for ventilation scenarios SC2 and SC4. Scenarios SC2 and SC4 had a square window opening of a size of 1.5 m and 1.0 m, respectively. These scenarios had a doorway of a size of 0.9 m wide and 2.0 m high located in the wall opposite to the window opening. The window opening size in scenario SC2 (2.25 m<sup>2</sup>) was 125% larger than that in scenario SC4 (1.0 m<sup>2</sup>); resulting in larger heat losses by convection and radiation in scenario SC2 than that in scenario SC4. Consequently, the average temperature in scenario SC4 was higher than scenario SC2. The temperature averaged over the period of post-flashover in scenario SC4 (896°C) was 317°C higher than in scenario SC2 (579°C). The onset of post-flashover took place at about the same time in both scenarios (~60 s). Additionally, the period of post-flashover in scenario SC4 was slightly longer than that in scenario SC2.

Figure 3-20 compares the average temperature and mass loss in the case of having both window opening and doorway located in the same wall in ventilation scenarios SC7 and SC8. These scenarios had the same doorway size (0.9 m wide and 2.0 m high) with different window opening sizes. As shown in this figure, the window opening size had an insignificant effect on both the average temperature and the onset of post-flashover and its period. The temperature averaged over the period of post-flashover in scenario SC7 (1.0x1.5 m window opening) (923°C) was only 20°C higher than in scenario SC8 (1.0x1.0 m window opening) (903°C). In both scenarios, the onset of post-flashover occurred at 63 s and its period was 168 s (from 63 – 231 s).

Figure 3-21 compares the average temperature and mass loss in the case of having only a doorway with different sizes as in ventilation scenarios SC5 (0.9x2.0 m doorway) and

SC6 (1.5x2.0 m doorway). As shown in this figure, for the same time, the average temperatures within the compartment in these scenarios were different. However, the temperature averaged over the period of post-flashover in the scenario with a larger doorway size (SC6) was slightly higher than in the scenario with a smaller doorway size (SC5). These temperatures were 852 and 836°C in scenarios SC6 and SC5, respectively. On the other hand, the onset of post-flashover occurred earlier with a shorter period in the scenario with a larger doorway size. The onset of post-flashover and its period in scenario SC6 were 63 s and 156 s (from 63 – 219 s), respectively, compared to 77 s and 201 s (from 77 – 278 s) in scenario SC5.

The last comparison of the average temperature and mass loss is shown in Figure 3-22 for the case of having two similar ventilation openings (2.0x1.5 m window opening) but with different fire load locations. The temperature averaged over the period of post-flashover in scenario SC3 with fire load located at the room center (885°C) was 170°C higher than that in scenario SC9 with fire load located at the northeast corner of the room (715°C). The onset of post-flashover in scenario SC3 occurred at 65 s, 30 s earlier than in scenario SC9 (95 s). Furthermore, the period of the post-flashover in scenario SC3 (174 s, from 65 – 239 s) was 40 s shorter than in scenario SC9 (214 s, from 95 – 309 s).

In summary, in the cases of having only a window opening as in scenarios SC1, SC3, SC10 and SC11, and a doorway and window opening facing each other as in scenarios SC2 and SC4, the window opening size had a significant effect on the temperature and both the onset of post-flashover and its period. However, in the case of having a window opening and doorway located in the same wall, the size of the window opening did not affect the temperature and both onset of post-flashover and its period as in scenarios SC7 and SC8.

In the case of having only a doorway as in scenarios SC5 and SC6, its size had a significant effect on the temporal change of the average temperature within the compartment and the onset of post-flashover and its period, but had an insignificant effect on the temperature averaged over the period of post-flashover. Moreover, the fire load location as in scenarios SC3 and SC9 had a significant effect on the temperature and the onset of post-flashover and its period.

## Comparison of post-flashover temperatures of different scenarios

Figure 3-23 shows the temperatures averaged over the period of post-flashover for all ventilation scenarios. As shown in this figure, a range of ventilation factor,  $\Psi$  ( $\Psi = A_o \sqrt{H_o} / A_T$ ) between  $\sim 0.01 - 0.08 \text{ m}^{1/2}$  was covered for a fire in a room of a size of 4.2 m long, 3.8 m wide and 2.4 m high. In all scenarios but SC9, the fire load was placed at the room center. In scenario SC9, however, the fire load was placed in the northeast corner of the room and located 100 mm from both the east and north walls (see Figure 1-6 and Table 1-1). As indicated earlier, for the same ventilation factor, changing the fire load location from the room center (SC3) to its corner (SC9) resulted in a decrease in the average temperature by  $170^\circ\text{C}$  (see Figure 3-23 and Table 3-4). As such, the fire load location has an effect not only on the heat release rate but also on the temperature inside the compartment.

In all ventilation scenarios with fire load located at the room center, increasing the ventilation opening(s) increased the average temperature within the range of ventilation factor from  $\sim 0.01 - \sim 0.05 \text{ m}^{1/2}$ . A further increase in the ventilation factor from  $\sim 0.05 - \sim 0.07 \text{ m}^{1/2}$  resulted in an insignificant effect on the average temperature. In this range of ventilation factor ( $\sim 0.05 - \sim 0.07 \text{ m}^{1/2}$ ), the average temperature was more or less constant and its mean value was  $\sim 890^\circ\text{C}$  (Figure 3-23). Accordingly, the range of ventilation factor from  $\sim 0.01 - \sim 0.07 \text{ m}^{1/2}$  represented the case of ventilation-controlled burning in a room of a size of 4.2 m long, 3.8 m wide and 2.4 m high. However, for ventilation factor greater than  $\sim 0.07 \text{ m}^{1/2}$ , the average temperature decreased with increasing the ventilation factor (see SC2 in Figure 3-23). As a result, a range of ventilation factor  $> \sim 0.07 \text{ m}^{1/2}$  represented the case of fuel-controlled burning in a room of a size of 4.2 m long, 3.8 m wide and 2.4 m high.

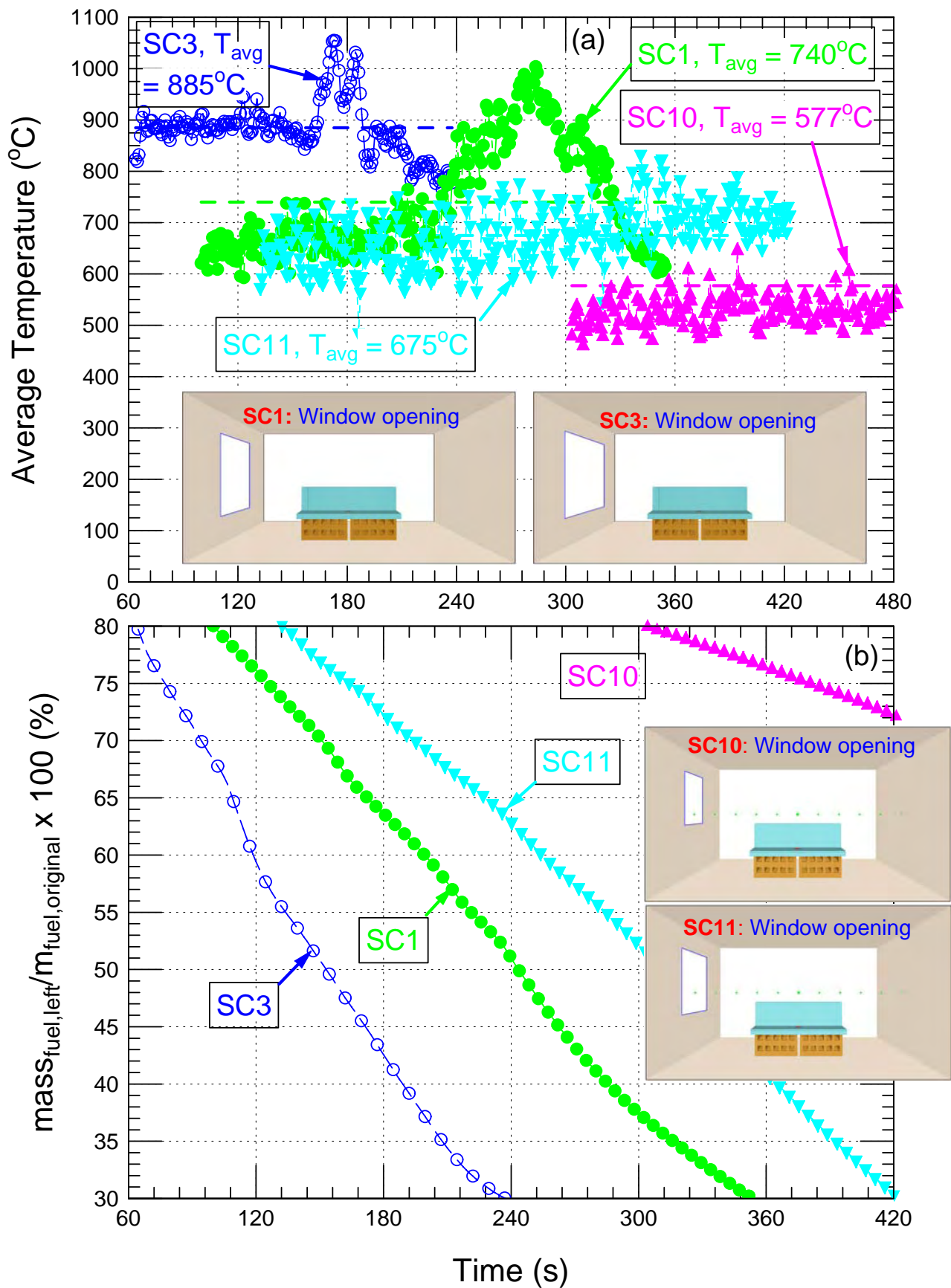


Figure 3-18 Comparison of the average temperatures and mass losses during the period of post-flashover for scenarios using a window opening with different sizes

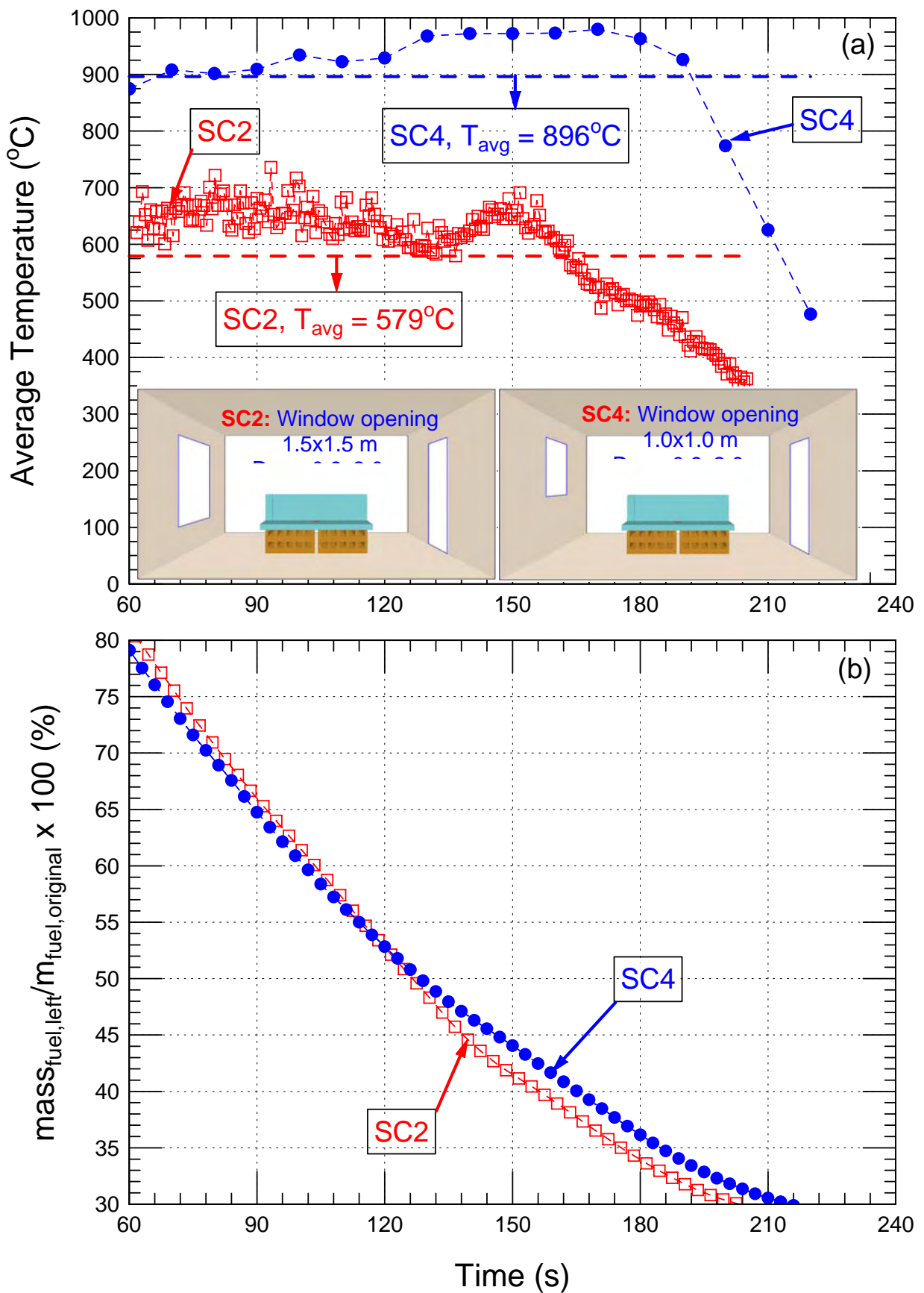


Figure 3-19 Comparison of the average temperatures and mass losses during the period of post-flashover for scenarios using window opening and doorway facing each other

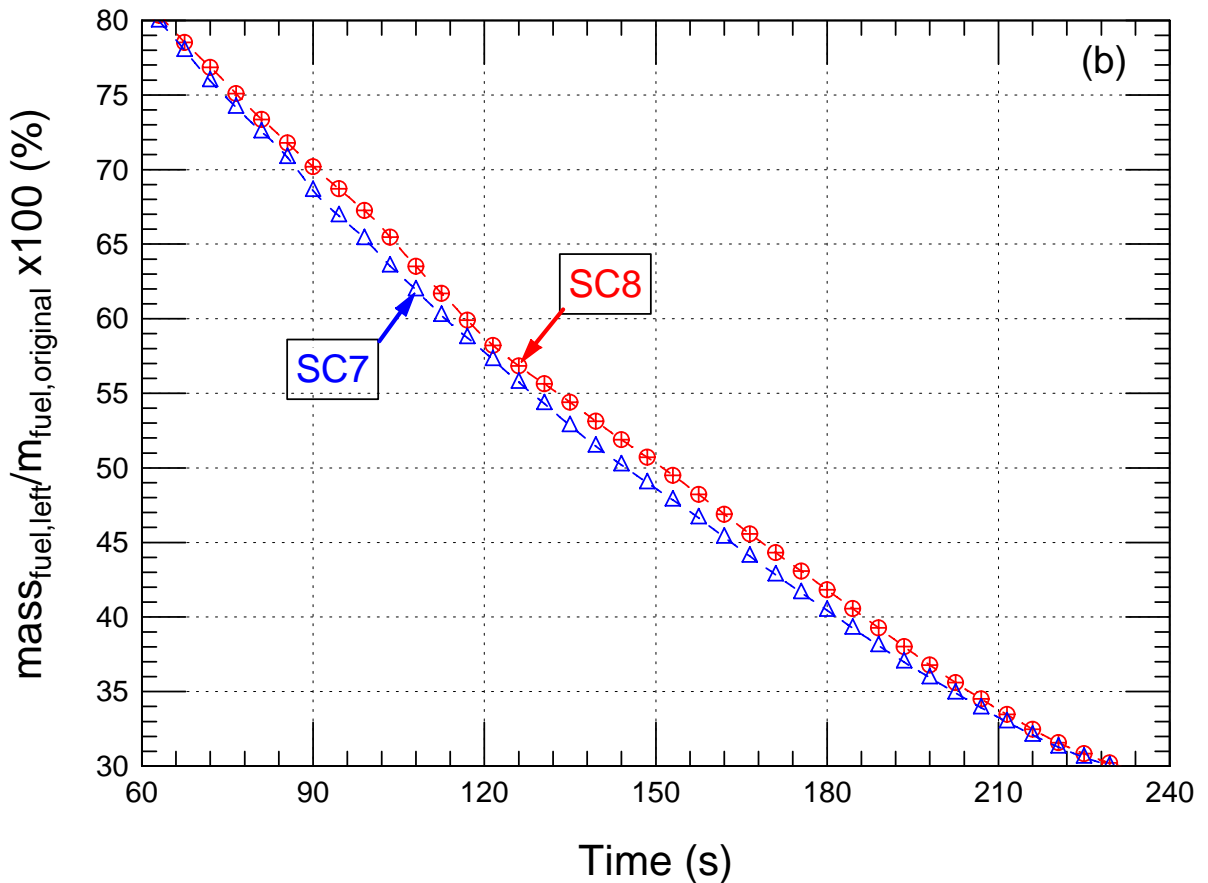
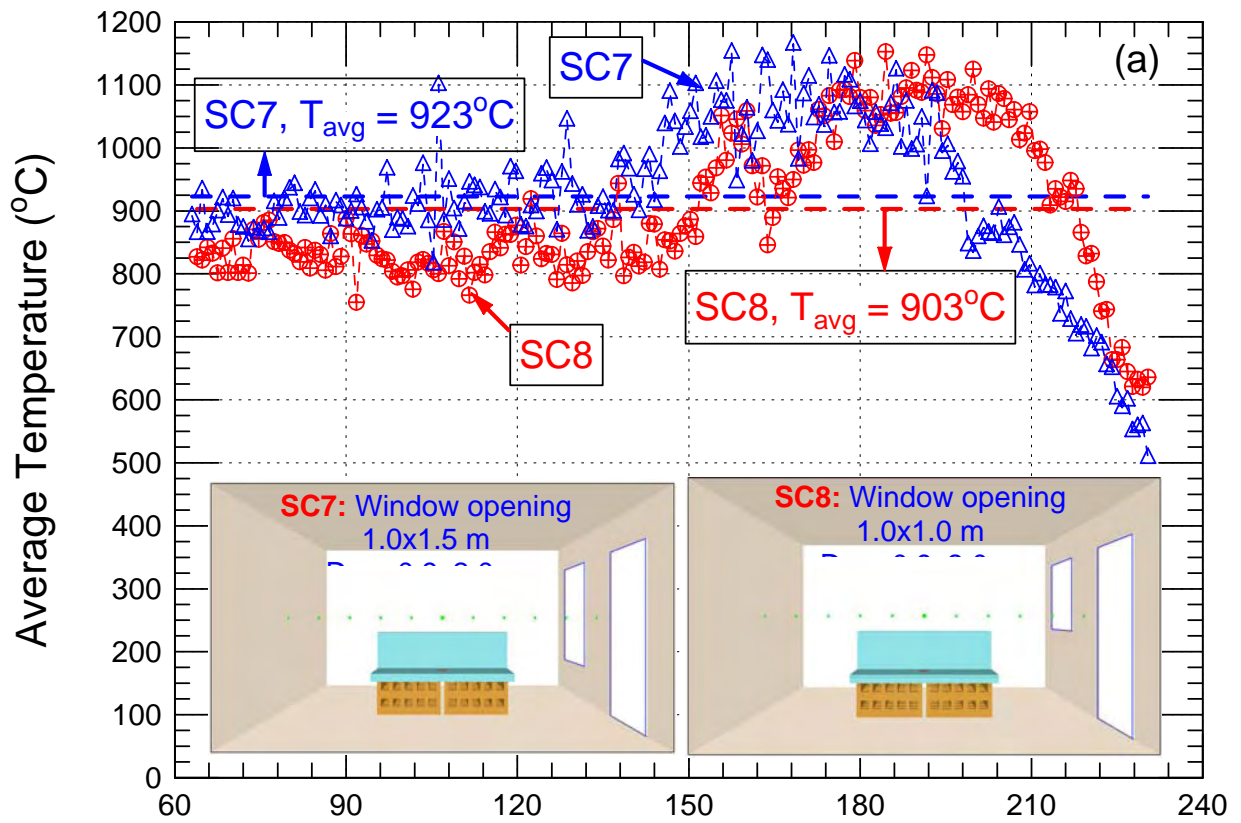


Figure 3-20 Comparison of the average temperatures and mass losses during the period of post-flashover for scenarios using window opening and doorway located in the same wall

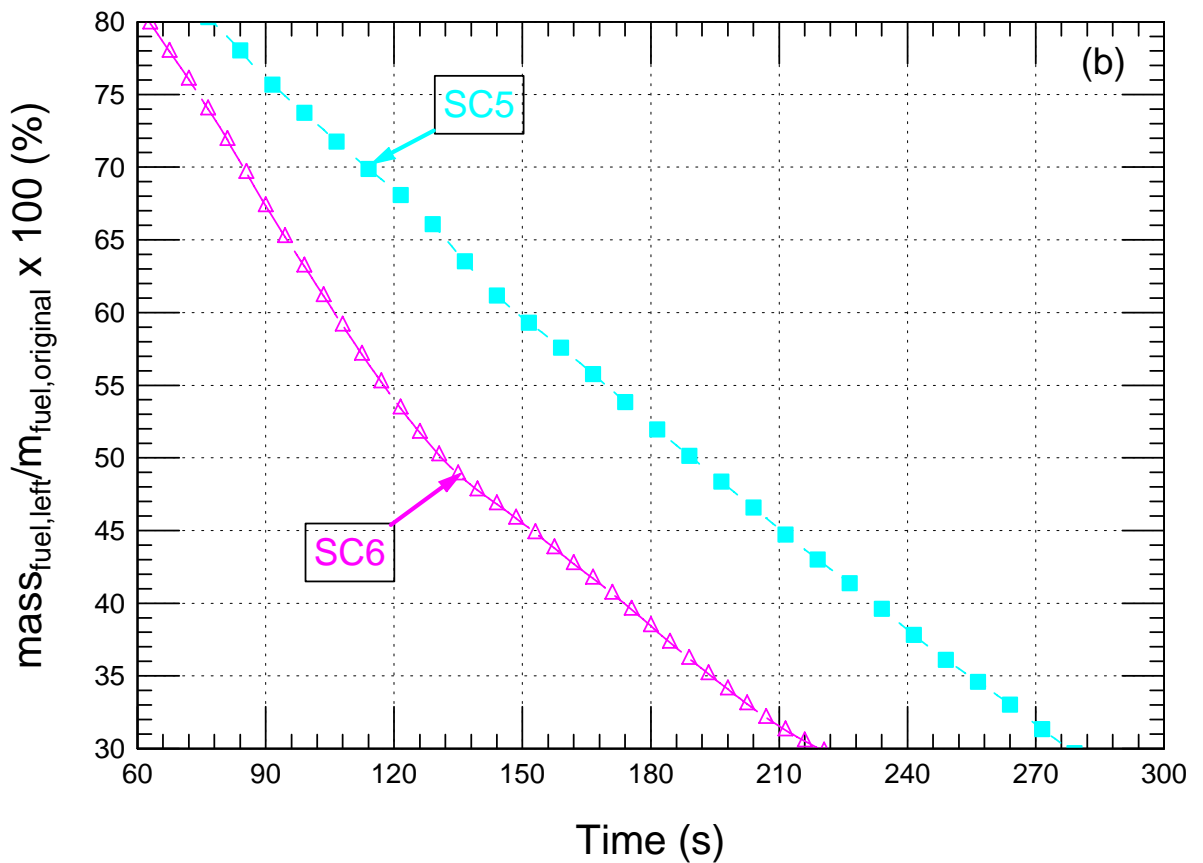
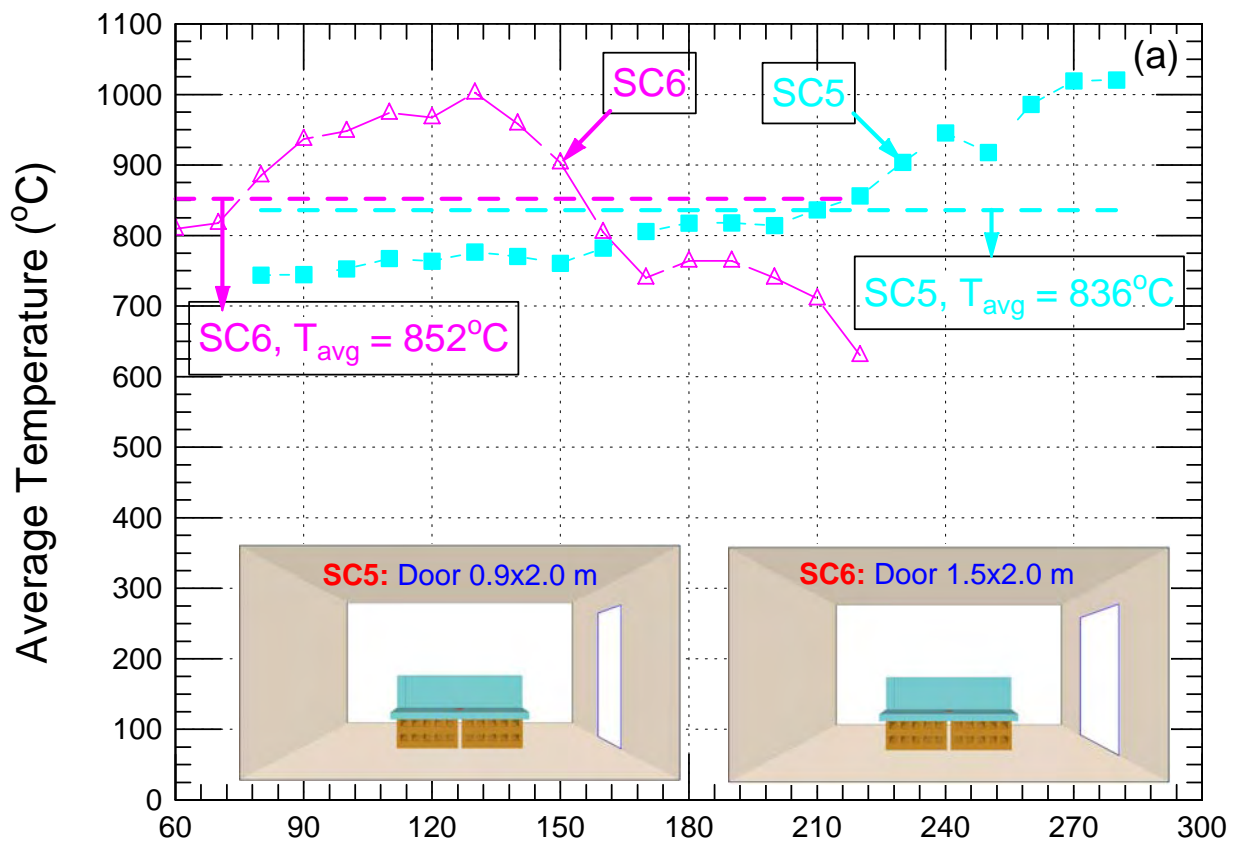


Figure 3-21 Comparison of the average temperatures and mass losses during the period of post-flashover for scenarios using doorway with different sizes

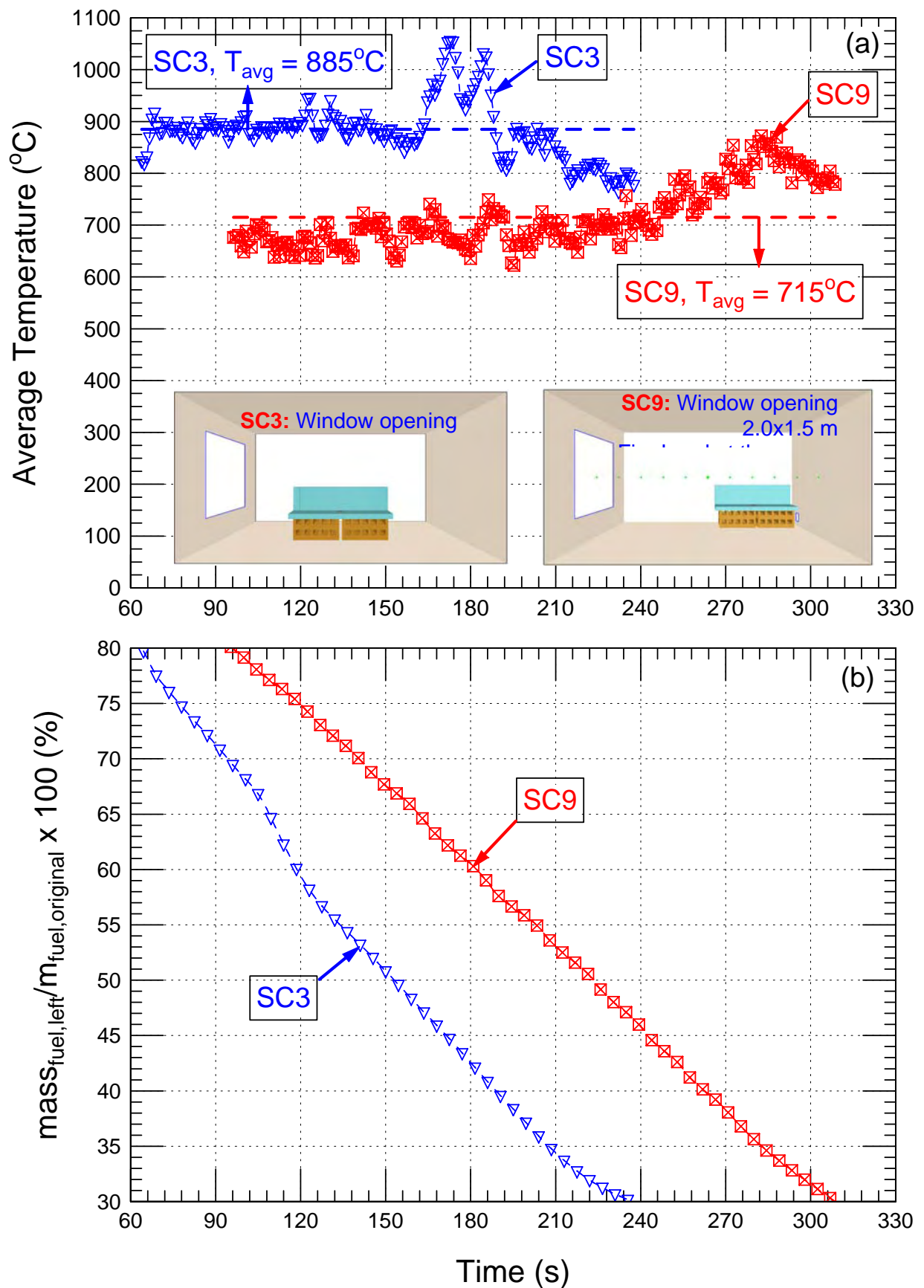


Figure 3-22 Comparison of the average temperatures and mass losses during the period of post-flashover for scenarios with different fire load locations

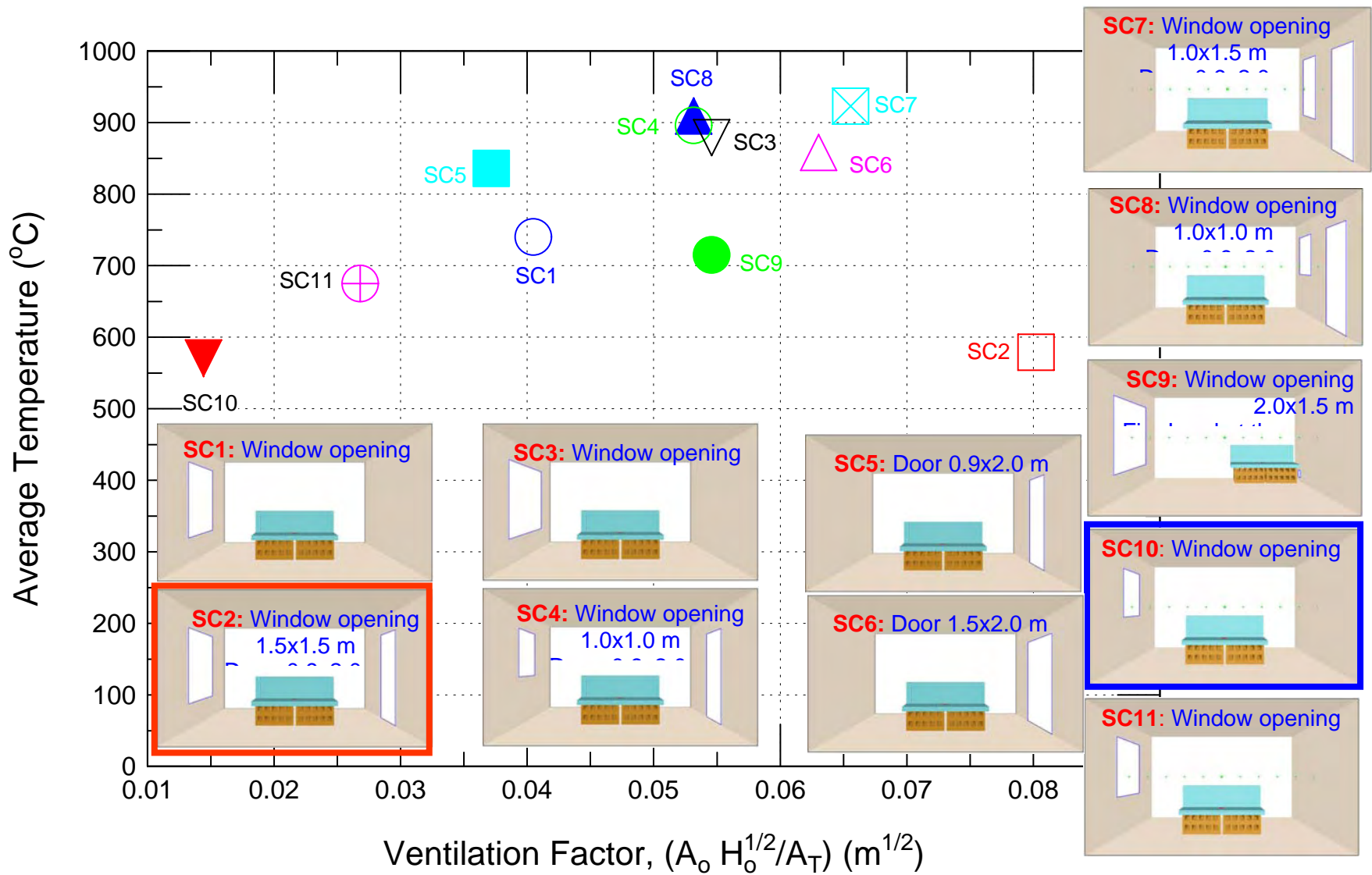


Figure 3-23 Average temperature of all ventilation scenarios over the period of post-flashover

## 4 Summary and Conclusion

Eleven ventilation scenarios were simulated using FDS version 5 in order to identify the proper ventilation scheme for conducting design fire tests in a room of a size of 4.2 m length x 3.8 m width x 2.4 m height. These scenarios covered a wide range of ventilation factor,  $\Psi$  ( $\Psi = A_o \sqrt{H_o} / A_T$ ) of  $\sim 0.01 - 0.08 \text{ m}^{1/2}$ . A fire load that consisted of a polyurethane sofa and two wood cribs underneath it was used in all scenarios. The total masses of the polyurethane sofa and two wood cribs were 8.3 kg and 86.7 kg, respectively. In all scenarios but SC9, the fire load was located at the room center. In scenario SC9, however, the fire load was located at the northeast corner of the room. The ventilation schemes in all scenarios were based on using exterior square/rectangular opening(s) to represent window opening, doorway, or both with different sizes. In all CFD simulations, it was assumed that the walls and ceiling of the compartment were perfectly insulated. This represented the most severe fire condition.

Before conducting the CFD simulations for all scenarios, many numerical tests and debugging were carried out in order to (a) find out the optimum mesh size, and (b) test the validity of the new combustion model in FDS version 5 (see reference [1]). More details about the fire characteristics are available in the previous report [1].

Comparisons of the CFD results of all ventilation scenarios were summarized in Table 3-1 through Table 3-4. The following observations were made from the CFD results of the eleven ventilation scenarios:

- Ventilation scenario SC8 had the highest peak heat release rate (7,450 kW).
- Ventilation scenario SC10 with the smallest ventilation factor had the lowest peak heat release rate (4,400 kW).
- The polyurethane sofa took the longest period to be completely burned in SC10 (779 s).
- The polyurethane sofa took the shortest period to be completely burned in SC2 (158 s).
- Ventilation scenario SC11 had the largest total mass loss (79.8 kg) (71.5 kg wood and 8.3 kg polyurethane sofa). Only 15.2 kg (18% by mass) of the wood was left when the fire was completely extinguished. This scenario had a 1.4 m wide and 1.2 m high rectangular window opening, which is the average size of window openings in multi-family dwellings based on a survey [3].
- Ventilation scenario SC2 had the lowest total mass loss (68.0 kg) (59.7 kg wood and 8.3 kg polyurethane sofa). At the time when the fire was completely extinguished, a 27.0 kg (31% by mass) of the wood was left in this scenario.
- Ventilation scenario SC10 with the smallest ventilation factor ( $\sim 0.01 \text{ m}^{1/2}$ ) had the longest period of burning. Combustion was still taking place with a heat release rate of  $\sim 1,500 \text{ kW}$  at the end of simulation (900 s).
- A range of ventilation factor of  $\sim 0.01 - \sim 0.07 \text{ m}^{1/2}$  was found to represent the case of ventilation-controlled burning in a room of size of 4.2 m long, 3.8 m wide and 2.4 m high.
- A ventilation factor greater than  $\sim 0.07 \text{ m}^{1/2}$  was found to represent the case of fuel-controlled burning in a room of size of 4.2 m long, 3.8 m wide and 2.4 m high.

- The window opening size had a significant effect on the fire characteristics in the cases of having (1) a window opening and doorway facing each other as in scenarios SC2 and SC4, and (2) only a window opening as in scenarios SC1, SC3, SC10 and SC11.
- In the case of having a window opening and doorway in the same wall as in scenarios SC7 and SC8, the size of the window opening had an insignificant effect on the fire characteristics.
- In the case of having only a doorway as in scenarios SC5 and SC6, the doorway size had a significant effect on the fire characteristics.
- The location of the fire load had a significant effect on the fire characteristics as in scenarios SC3 and SC9.
- Because the heat losses through the room boundaries were neglected (walls and ceiling were assumed to be fully insulated to represent the most severe fire condition), the present CFD predictions for the temperature averaged over the period of post-flashover of different ventilation scenarios were higher ( $\leq +25\%$ ) than that obtained using Babrauskas' correlation [11].

## 5 References

1. Saber, H. H., Kashef, A., Bwalya, A., Lougheed, G. D., and Sultan, M. A., A Numerical Study on the Effect of Ventilation on Fire Development in a Medium-Sized Residential Room, Research Report # IRC-RR-241, National Research Council of Canada, Ottawa, Canada, February 2008.
2. Saber, H. H., and Kashef, A. "CFD Simulations for Different Fire Ventilation Scenarios in a Room", 5<sup>th</sup> NRC Symposium on Computational Fluid Dynamics and Multi-scale Modelling, Ottawa, Canada, January 2008.
3. Bwalya, A., Lougheed, G., Kashef, A., and Saber, H. H. "Survey Results of Combustible Contents and Floor Areas in Multi-Family Dwellings", National Research Council of Canada, Institute for Research in Construction, Ottawa, Research Report IRC-RR-253, 2008.
4. Bwalya, A., Carpenter, D., Kanabus-Kaminska, M., Lougheed, G., Su, J., Taber, B., Benichou, N., Kashef, A., McCartney, C., Bounagui, A., and Thomas, R. "Development of A Fuel Package for Use in the Fire Performance of Houses Project" Research Report: IRC-RR-207, March 2006.
5. Taber, B., Bwalya, A., McCartney, C., Bénichou, N., Bounagui, A., Carpenter, D., Crampton, G., Kanabus-Kaminska, M., Kashef, A., Leroux, P., Lougheed, G., Su, J., and Thomas, R. "Fire Scenario Tests in Fire Performance of Houses Test Facility – Data Compilation" Research Report: NRC-IRC-RR-208, March 2006.
6. McGrattan, K., Baum, H., Rehm, R., Hostikka, S., and Floyd, J., "Fire Dynamics Simulator (Version 5) Technical Reference Guide", NIST Special Publication 1018-5, October 2007.
7. McGrattan, K., Klein, B., Hostikka, S., and Floyd, J., "Fire Dynamics Simulator (Version 5) User's Guide" NIST Special Publication 1019-5, October 2007.
8. Hurley, M. J., "Evaluation of Models of Fully Developed Post-flashover Compartment Fires", *Journal of Fire Protection Engineering* vol. 15; pp. 173-197, 2005.
9. Walton, W. D., and Thomas, P. H., "Estimating Temperatures in Compartment Fires", section three, Chapter 6, *The SFPE Handbook of Fire Protection Engineering*, 3<sup>rd</sup> Edition, 2002.
10. Babrauskas, V. and Williamson, R. B., "Post-flashover Compartment Fires- Application of a Theoretical Model", *Fire and Materials*, vol. 3, no. 1, pp. 1-7, 1979.
11. Babrauskas, V., "A Closed-form Approximation for Post-flashover Compartment Fire Temperatures", *Fire Safety Journal*, vol. 4, pp. 63-73, 1981.

## **6 Appendix–A: Average Temperatures and Mass Losses within the Period of Post-flashover for all Ventilation Scenarios**

Appendix – A includes a set of figures for some of the results of the numerical simulations of the eleven ventilation scenarios. These results include:

- The average temperature within the compartment during the period of fully-developed fire (post-flashover),
- The temperature averaged over the period of post-flashover, and
- The mass loss of the fire load during the period of post-flashover.

The full description of eleven fire scenarios is available in the main body of the report.

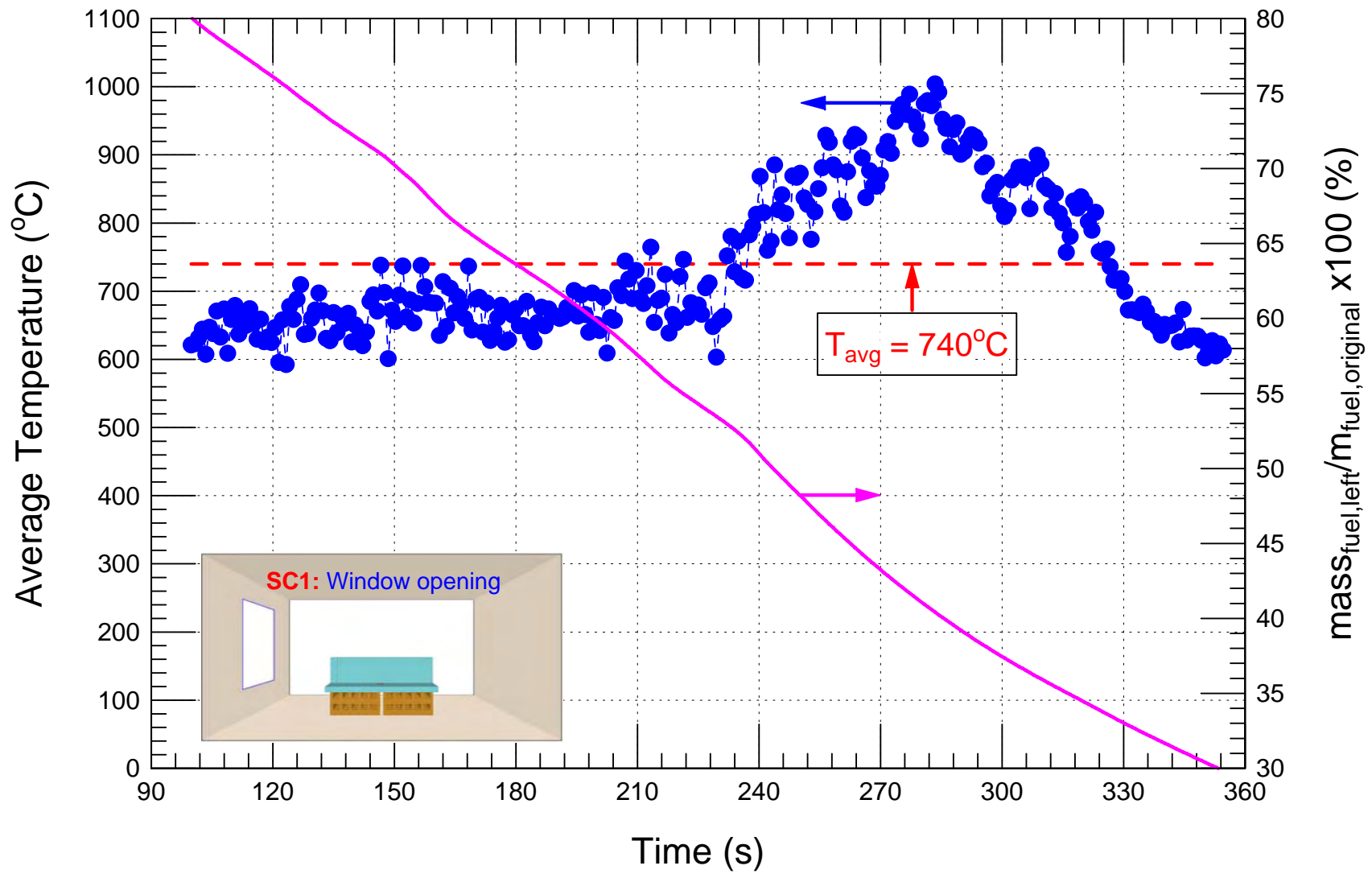


Figure 6-1 Temperature and mass loss during the period of post-flashover for ventilation scenario SC1

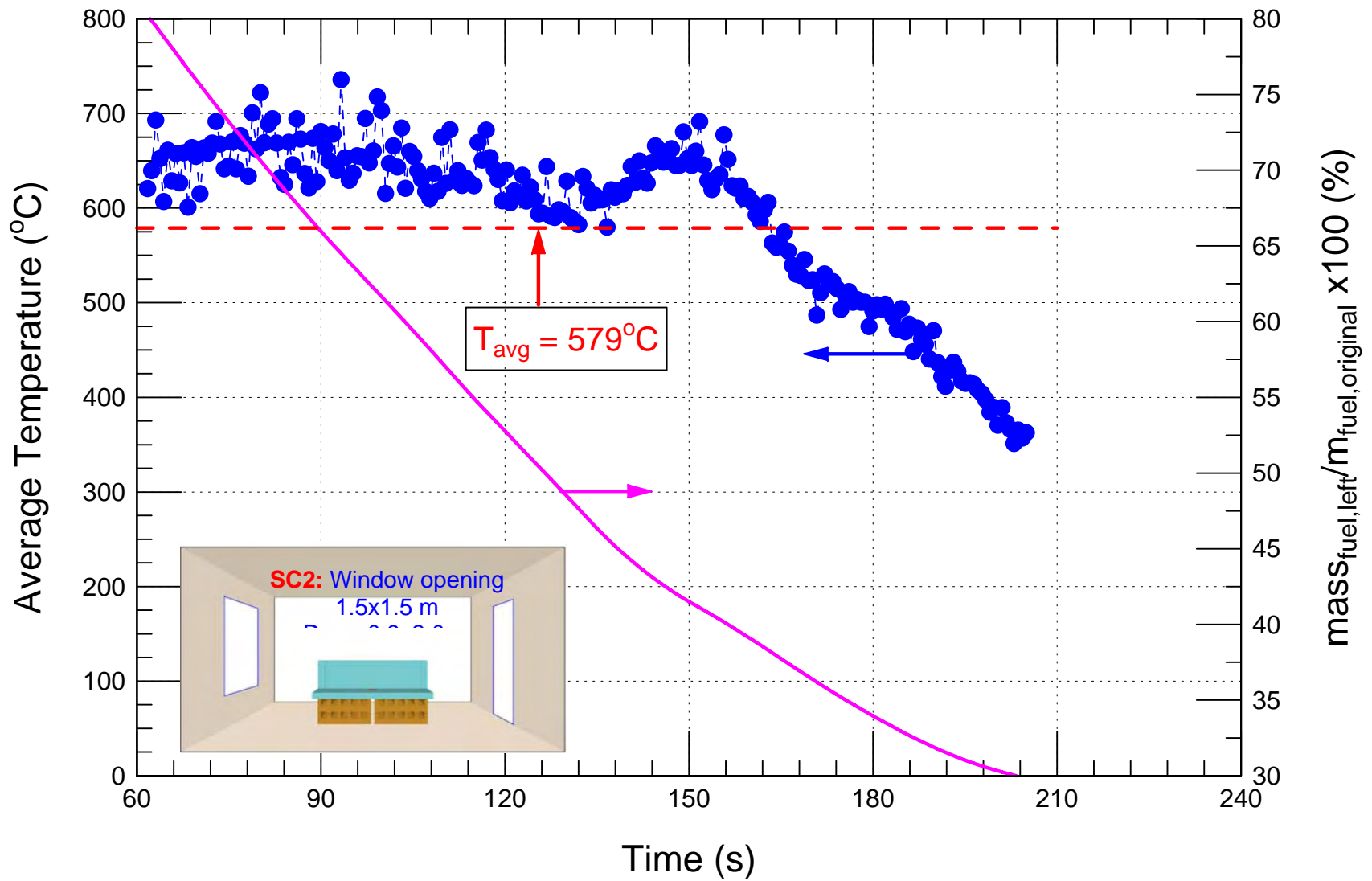


Figure 6-2 Temperature and mass loss during the period of post-flashover for ventilation scenario SC2

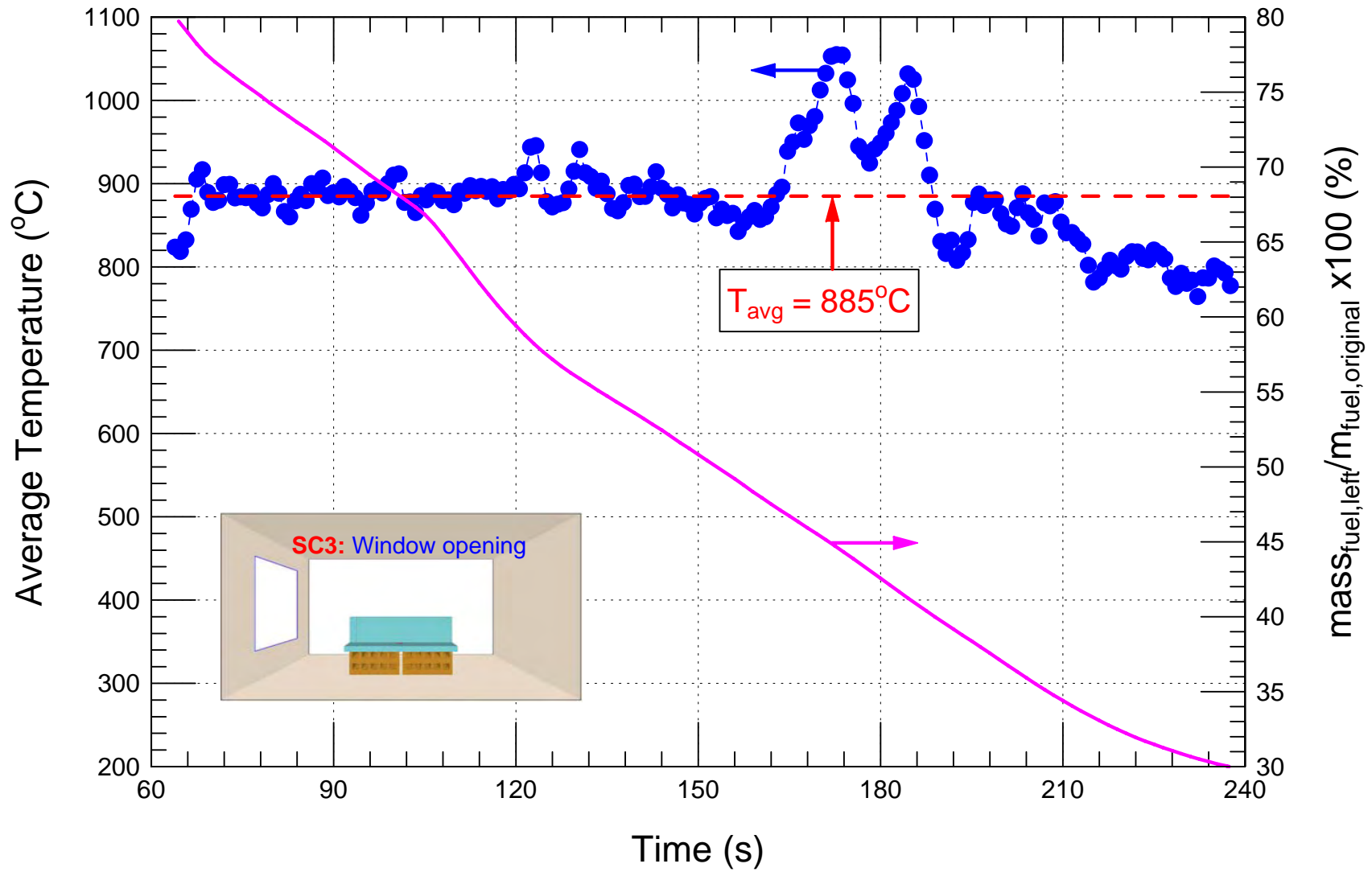


Figure 6-3 Temperature and mass loss during the period of post-flashover for ventilation scenario SC3

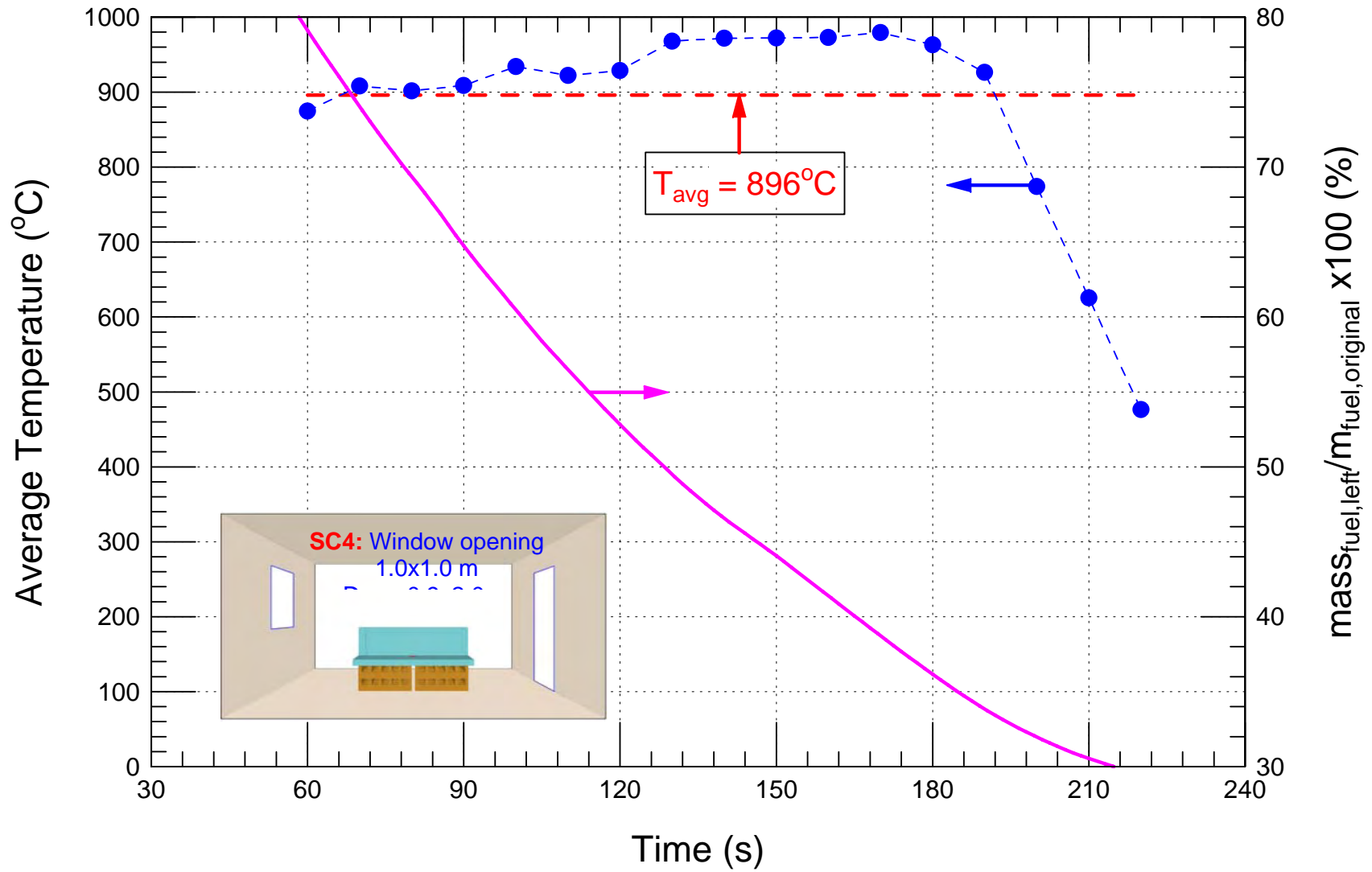


Figure 6-4 Temperature and mass loss during the period of post-flashover for ventilation scenario SC4

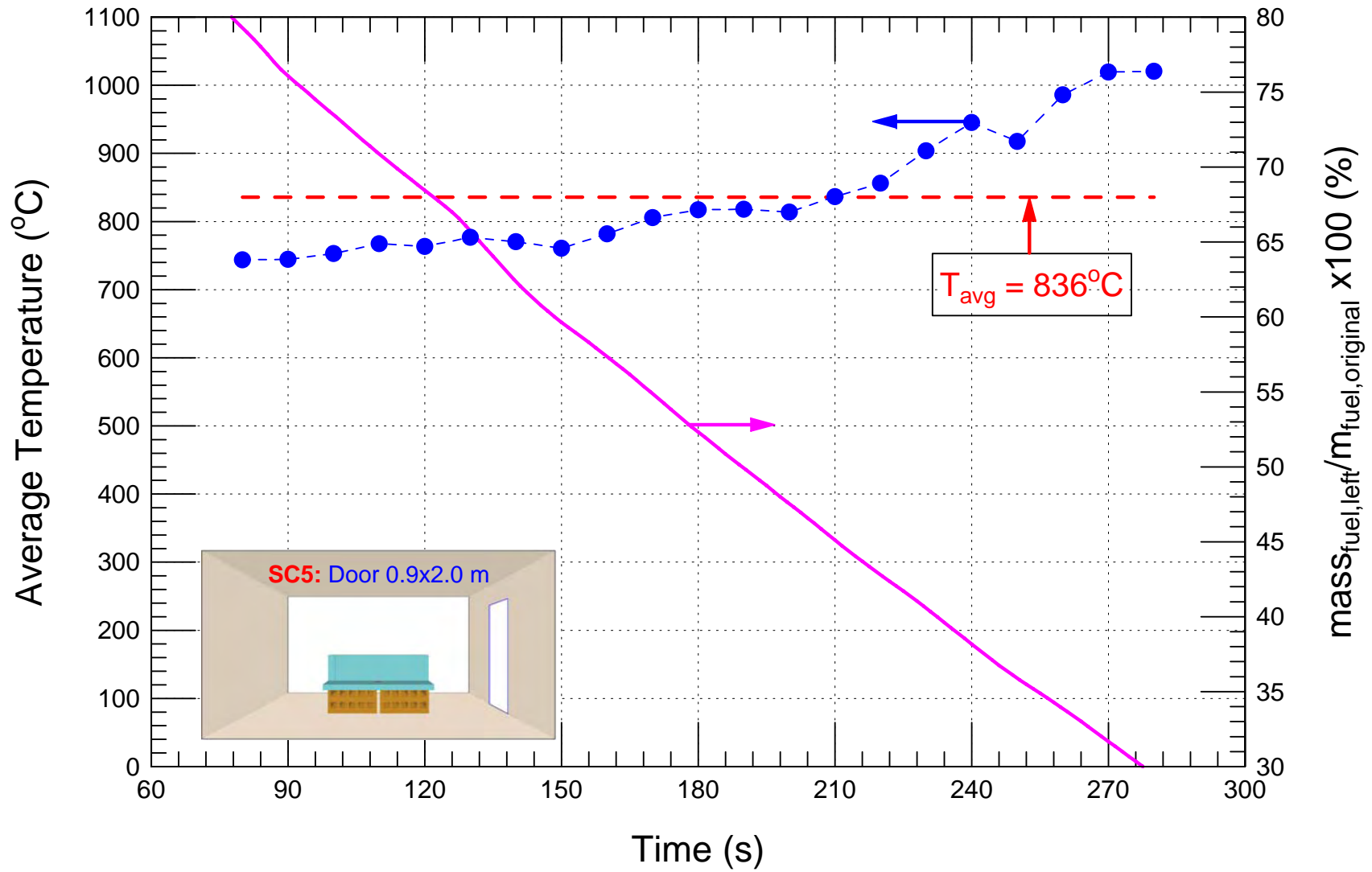


Figure 6-5 Temperature and mass loss during the period of post-flashover for ventilation scenario SC5

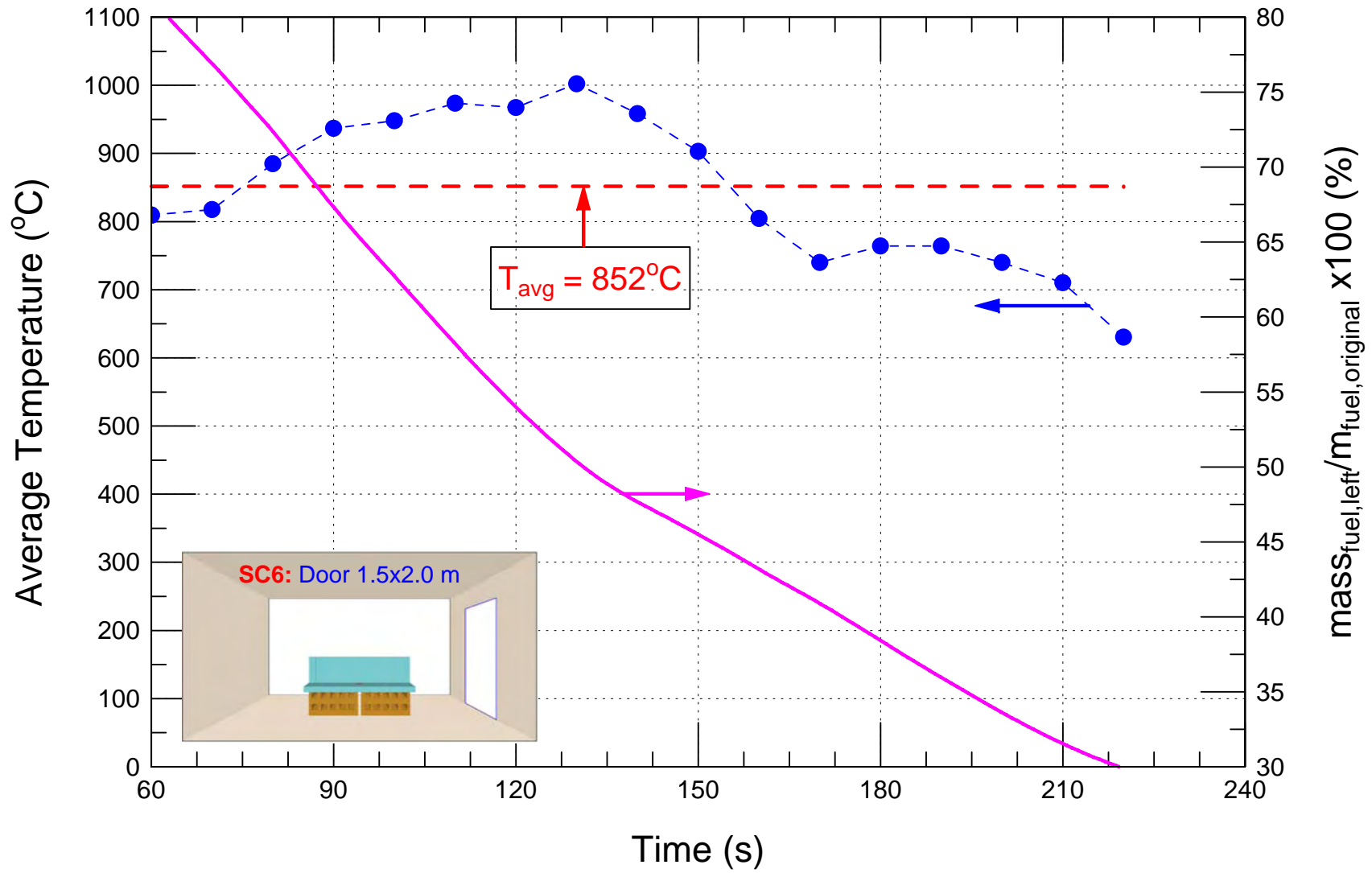


Figure 6-6 Temperature and mass loss during the period of post-flashover for ventilation scenario SC6

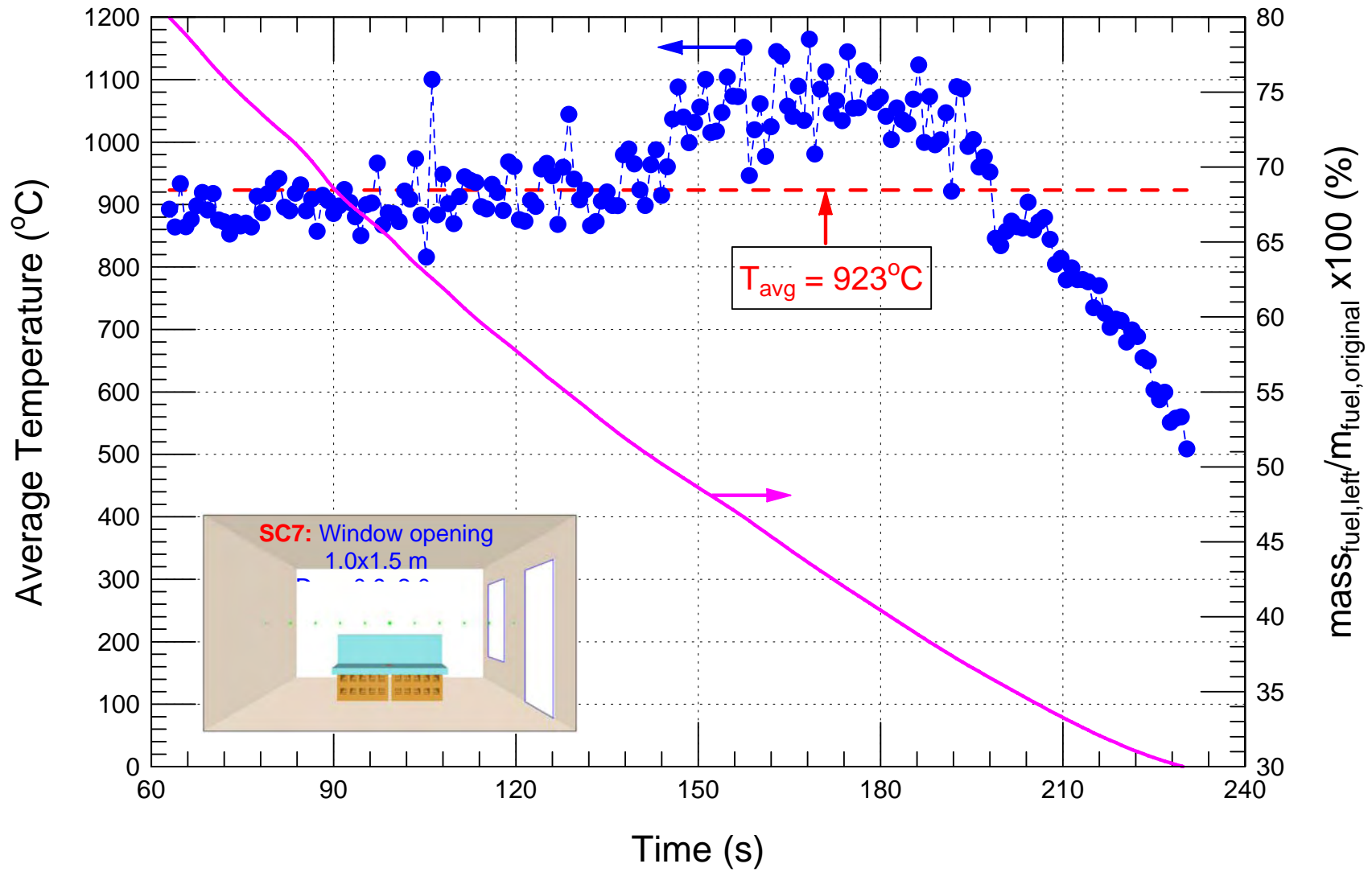


Figure 6-7 Temperature and mass loss during the period of post-flashover for ventilation scenario SC7

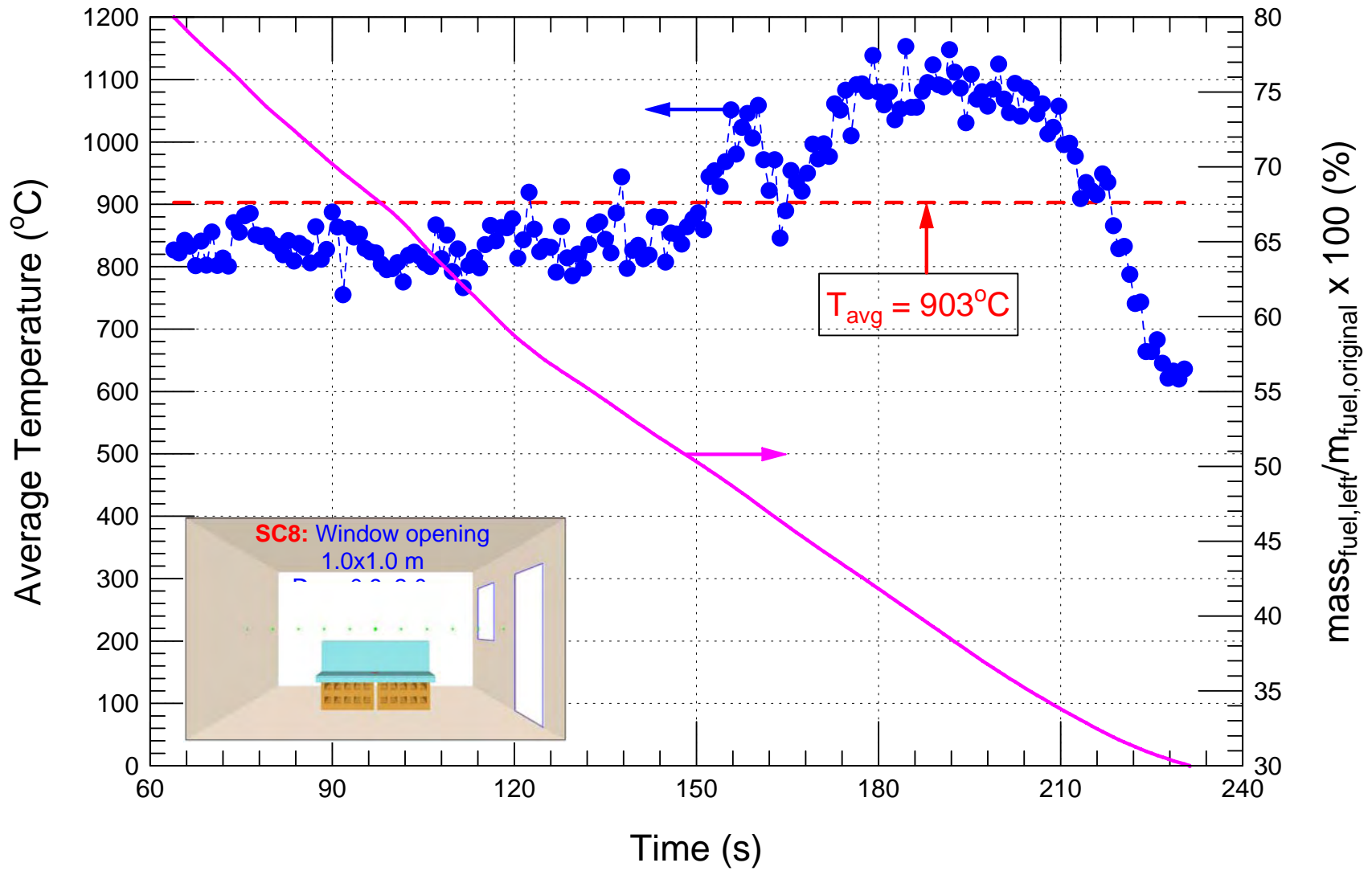


Figure 6-8 Temperature and mass loss during the period of post-flashover for ventilation scenario SC8

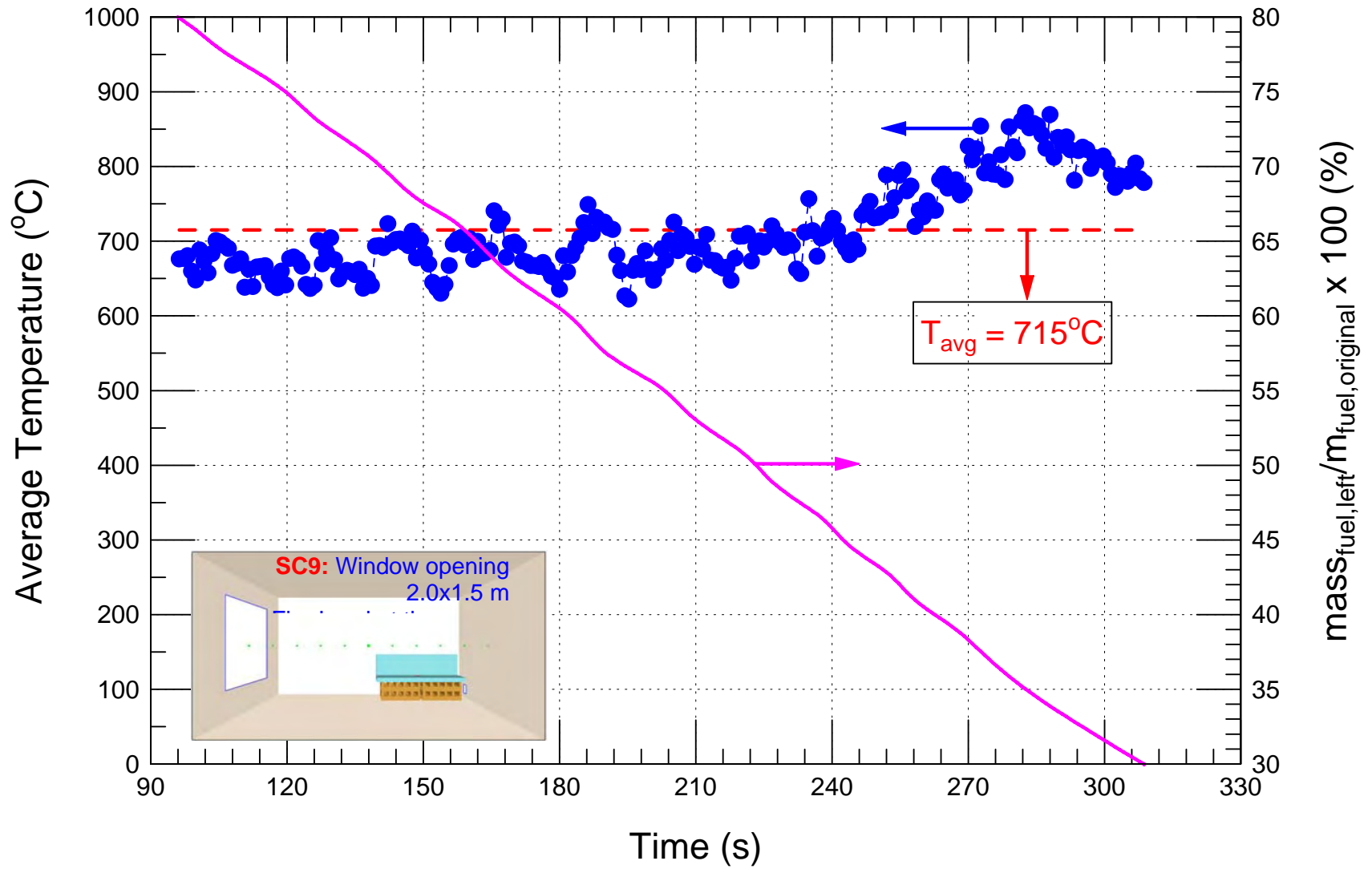


Figure 6-9 Temperature and mass loss during the period of post-flashover for ventilation scenario SC9

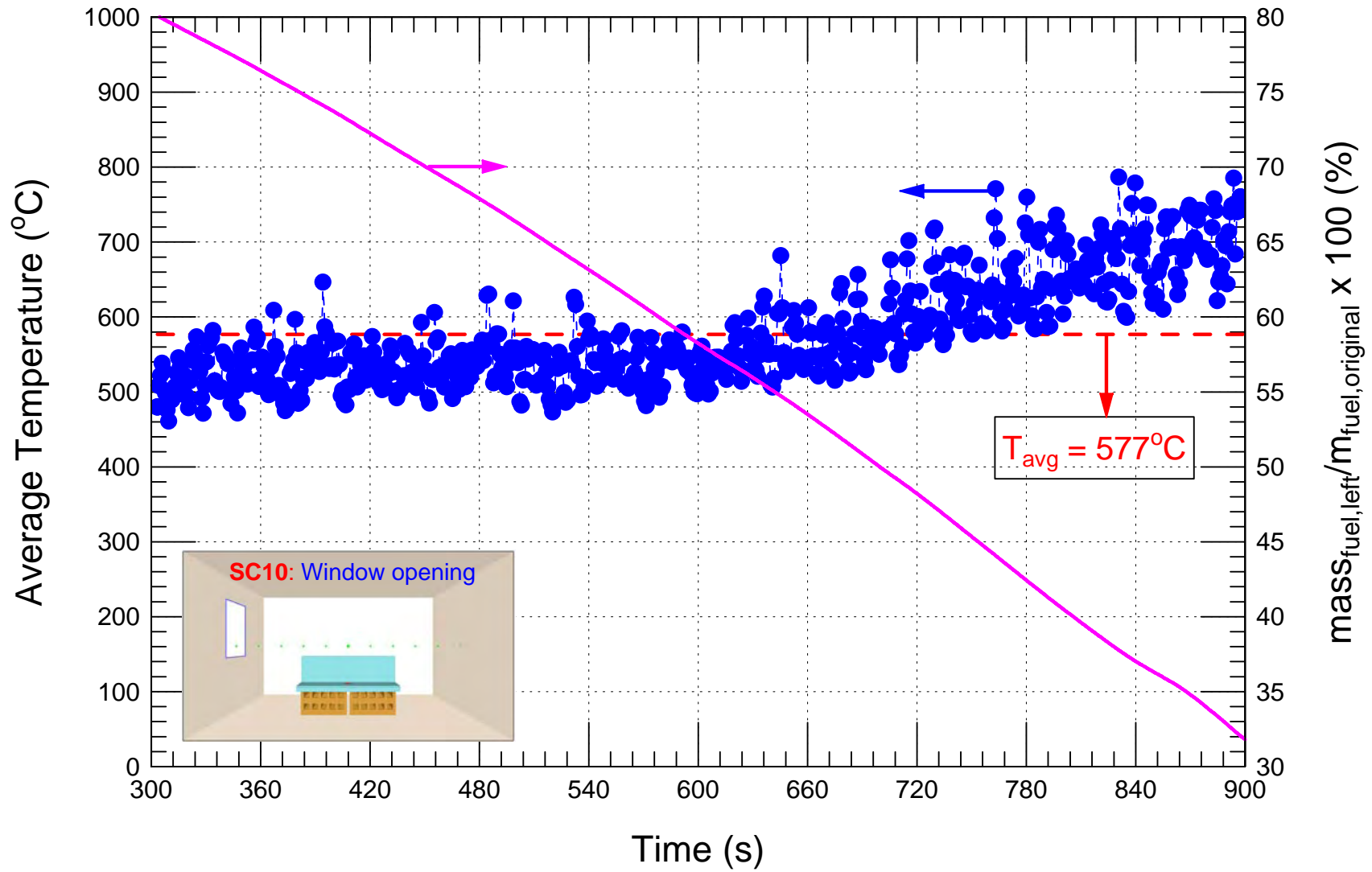


Figure 6-10 Temperature and mass loss during the period of post-flashover for ventilation scenario SC10

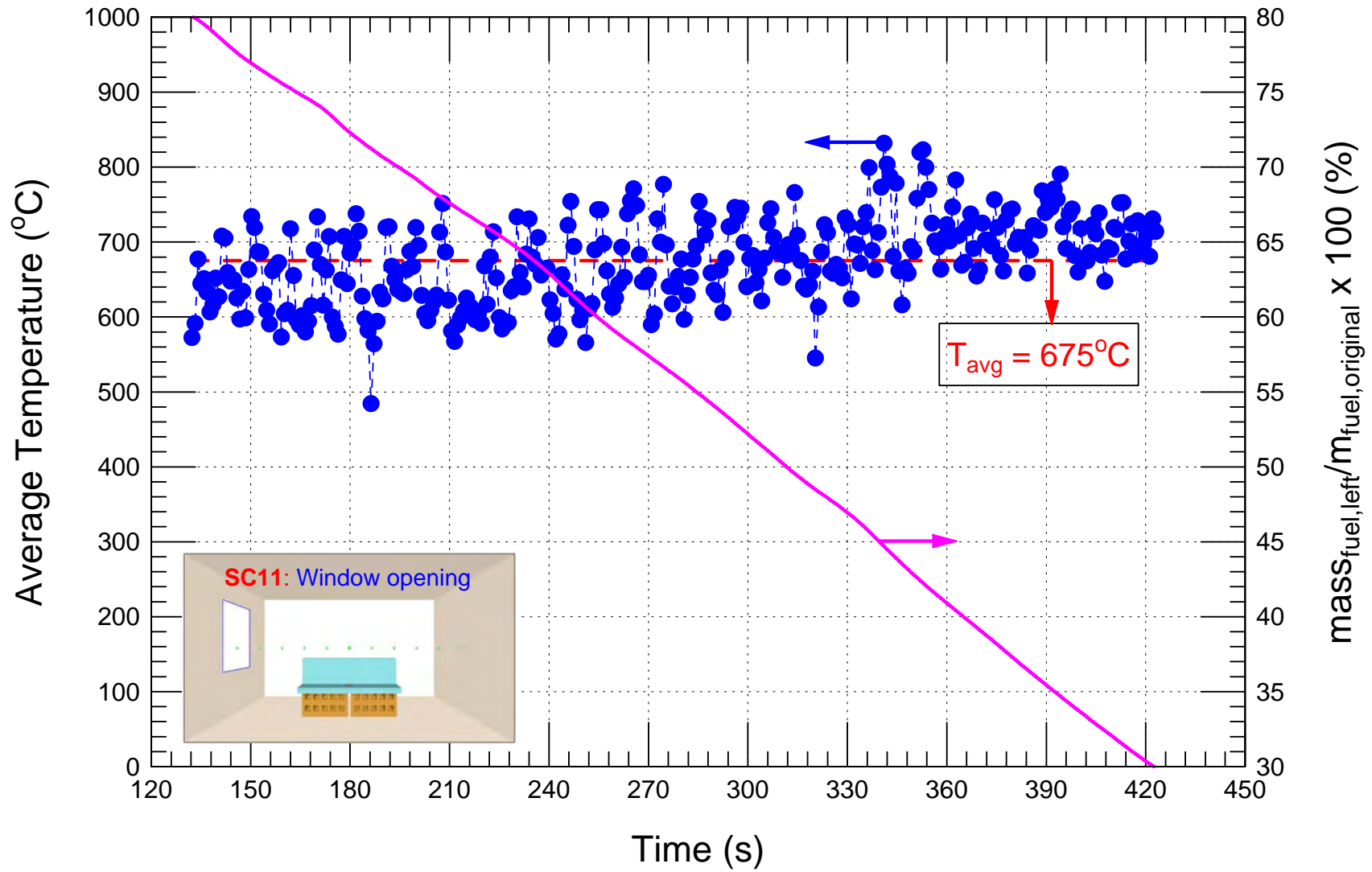


Figure 6-11 Temperature and mass loss during the period of post-flashover for ventilation scenario SC11